Universidad Autónoma de Madrid
Departamento de Física Teórica

UAM
Universidad Autónoma de Madrid

Double-copy structure in the high-energy regime: From QCD to gravity

Josep Rubí Bort

Director

Prof. Dr. Agustín Sabio Vera

Tutor

Prof. Dr. Julio Parra Martínez

Master thesis in Theoretical Physics

Academic year 2024 - 2025

Abstract

The double-copy structure is a state-of-the-art topic that has generated considerable interest in recent years. Its origin lies in string theory, through the Kawai-Lewellen-Tye (KLT) relations, but it has also been identified more recently in quantum field theory via the Bern-Carrasco-Johansson (BCJ) duality, which relate amplitudes in Yang-Mills theories to those in quantum gravity. In the first section, I review this process and discuss how perturbative quantum gravity can be treated. I then focus on the energy regime that is central to this thesis, highlighting the emergence of Reggeized gluons and gravitons, and reviewing the approximations and parametrizations relevant to this regime. Finally, I present a bottom-up approach to the double-copy structure by explicitly computing amplitudes in QCD and quantum gravity in order to extract the effective vertices that reveal this relation. These computations are carried out with the aid of Mathematica code that I developed specifically for this thesis. The thesis concludes by assessing whether the objectives have been achieved, discussing potential applications, and outlining possible future directions.

Objectives

The objectives of this thesis are the following:

1. Introduce the concept of the double-copy structure, identify where it appears, and examine how it emerges in different formalisms.

2. Introduce the Multi-Regge Kinematics limits via hadron scattering, and define the concepts of gluon and graviton reggeization.

3. Reproduce the results of [12] using Mathematica libraries. The code should enable faster computations and allow replication of similar, more complex results.

Contents

1 Introduction to the double copy structure

This section discusses the concept of the double-copy structure. Not only will the realization in Quantum Field Theories (QFT) be presented, but also a brief comment on how it is seen in string theory will be made. The section also examines the role of supersymmetry (SUSY) in this context and includes a brief introduction to it. The construction of perturbative quantum gravity will be presented at the end. Furthermore, some interesting problems in the context of quantum gravity that were found during the computation will be mentioned.

1.1 The basics of the double copy structure

In QFT, some authors discovered a relation called the color-kinematic duality, or also known as the BCJ duality (for its authors, Bern, Carrasco and Johanson). This duality states that when computing gauge amplitudes, one can change the colour factor for a kinematic factor, giving rise to a gravity amplitude ([1, 2, 3]). As an example, consider a gauge amplitude of the form

$$A_{gauge} = \alpha^3 \sum_i \frac{n_i c_i}{d_i} \tag{1.1}$$

where the sum is over all the possible diagrams, α is the gauge coupling constant, n_i is the numerator, c_i the color factor, and d_i the denominator all of the ith diagram. Then, the corresponding gravity amplitude can be written as

$$A_{gravity} = (\alpha')^3 \sum_i \frac{n_i \tilde{n}_i}{d_i}, \tag{1.2}$$

where α' is the coupling constant of gravity. Although this is the main conceptual foundation, the results of this thesis proceed via a bottom-up approach. Thus, further detail about the BCJ duality is omitted[I].

Not only does the BCJ duality apply to QCD and gravity, but also to theories with supersymmetries. It is interesting as it lets us simplify some of the calculations done in these supersymmetric theories. In Sect. 1.1.1 they are introduced with more detail. The interest about including SUSY is discussed in Sect. 1.1.2.

By moving to string theories, somewhat similar, but unrelated, relations are found. At the tree-level, Kawai, Lewellen and Tye (KLT) developed some relationships to compute scattering amplitudes. These express closed string amplitudes in terms of open string amplitudes. It is known that string theory at low energy reduce to QFT theories ([4]), enabling us to extract some information from that. As an example, in this limit one can relate the closed string to gravitons, while open strings would be connected to gauge threories ([5]). This means that at tree level, gravity amplitude must be expressible as a product of non-Abelian gauge-theory amplitudes. As already stated, the KLT method only works at tree-level, and to go further than that one needs to use other methods such as unitarity and dispersion relations (In Sect. 6.1 a bit more of this topic is brought up, but not much, since it is not directly related to the thesis objective.).

[I] For the interested reader, the detail can be found in [1, 2, 3] and much more papers talking about it.

1.1.1 Supersymmetries

Although it will not be used directly in this thesis, SUSY is of great interest in the community and is therefore briefly introduced here. Let us now examine the concept of SUSY from the point of view of QFT. To explain SUSY one needs to see the theorem of Coleman and Mandula ([6]). This theorem, roughly speaking, states that in any space-time of dimension bigger than 1+1, the only possible symmetries are

$$\text{Poincaré} \times \text{Internal}.$$

Internal means any other symmetry that is not Poincaré, for example, hypercharge. In the proof of such a theorem, there are two loopholes. One is the conformal invariance, and the other is SUSY. Conformal invariance will be omitted, as it is not relevant for this thesis. Although SUSY provides a richer framework, not much about them will be mentioned, as no significant lesson would be obtained for the purposes of this thesis. The reasons for working with QCD and EH gravity for this thesis are presented in Sect. 1.2.

Having established that supersymmetries naturally arise in QFT, one would like to know what exactly is SUSY. This comes from the modification of the Poincaré algebra, to the so-called super Poincaré algebra ([5, 7]). These modifications consists of adding new generator, which will be antihermitian. This may appear unusual, as it is far more common to work with hermitian generators for the Poincaré algebra. These generators modify the spectrum, introducing new particles—superpartners. The last detail to mention is the maximum number of antihermitian generators that one can add. In the case of dimension 4, this limits is $\mathcal{N} = 8$ generators. Further detail can be found in [7].

1.1.2 Cases of interest

Supergravity (SUGRA) with $\mathcal{N} = 8$ is a case of special interest. The double-copy of this case arises from two MSYM theories (Maximally Supersymmetric Yang-Mills, i.e., with $\mathcal{N} = 4$). What makes this maximally supersymmetric SUGRA so special is that it is yet to be proven to be UV divergent at any loop further than four([8, 9, 10]). Also, MSYM theories have high interest in the community, as their coupling does not run with the energy, and thus, they do not have the confinement, as it happens with QCD. Apart from this case, which is the one of most interest, there exists other such relations ([11]). For example, SUGRA with $\mathcal{N} = 4$ can be thought of as an MSYM and a normal YM (i.e., one with $\mathcal{N} = 4$ and another one with $\mathcal{N} = 0$) as its double-copy structure.

1.2 QCD and MSYM

As explained, the most interesting case is that of SUGRA $\mathcal{N} = 8$, which is the double copy of two MSYM. However, in [12], the basis for this thesis, works with QCD and not MSYM. The differences between both theories (MSYM and QCD) are considerable. Although both are Yang-Mills theories theories, MSYM has conformal invariance, while QCD does not. On top of this, the spectra differ when quarks are included. The quarks in the MSYM are in the adjoint representation while the ones in QCD are in the fundamental. Nevertheless, the gluonic sectors are largely similar. Diagrams with only gluons as external particles should have the same results

in both theories, at tree-level. Since the vertices connecting quarks and gluons have always two quark lines, the only possible difference in the gluon diagrams of both theories is at the loop-level. ([13, 14]). Something similar happens for SUGRA.

For this reason, the relation investigated in this thesis is restricted to gluons and gravitons only. This ensures that working with QCD and EH gravity at tree level is sufficient, while still capturing the relevant double-copy structure. In Appendix. A the QCD Feynman Rules (FR) are found.

1.3 Gravity quantization

It has been suggested that to find the double copy structure of gravity a very special type of Lagrangian should be considered ([15]), in which indices remain distinct and do not contract with each other. In terms of the metric components $g_{\mu\nu}$ the index μ and the index ν represent different "worlds", which should not mix. Thus, terms as h^{μ}_{μ} are forbidden. As an example, the quadratic term in a De Donder gauge is given by

$$\mathcal{L}_2 = -\frac{1}{2}h_{\mu\nu}\partial^2 h^{\mu\nu} + \frac{1}{4}h\partial^2 h, \tag{1.3}$$

where $h \equiv h^{\mu}_{\mu}$. However, this reasoning is not common to all the community working on this, so it will not be taken into account. What will be done is consider the Einstein-Hilbert Lagrangian for gravity and couple it to some scalars[II]. The action for the Hilbert-Einstein gravity coupled to the two scalars is given by

$$S_{EH} = \int d^4x\sqrt{-g}\left(-\frac{2}{\kappa^2}R + \frac{1}{2}g^{\mu\nu}\partial_\mu\phi\partial_\nu\phi + \frac{1}{2}g^{\mu\nu}\partial_\mu\Phi\partial_\nu\Phi\right), \tag{1.4}$$

where ϕ and Φ are the two scalars under consideration. On top of that, the gauge chosen is the De Donder, as it is the one where some of the vertices used in this thesis are the most simple. Despite that this is the case, in Appendix. B it is seen that one of them is still large. Although the procedure to obtain the FR will not be mentioned, some important facts will be highlighted.

The first question that arises is how gravity is quantized by making use of perturbation theory. The answer is quite simple, the metric tensor is split into a background and the perturbation as

$$g_{\mu\nu} = \eta_{\mu\nu} + \kappa h_{\mu\nu}. \tag{1.5}$$

Despite the fact that different notations arise in the community, such as the use of $-\kappa$ or 2κ, the end result is the same. What matters is to know that $\eta_{\mu\nu}$ is the background, while $h_{\mu\nu}$ are the perturbations, as usually. These perturbations are the so-called gravitons. However, difficulties emerge at this point. The first thing to notice is that in Eq. (1.4) the metric determinant is present. The nonlinearity of it will bring some major issues. The exact powers of h present can be found through the relation

$$\mathrm{Det}[e^A] = e^{\mathrm{Tr}\{A\}} \xrightarrow{e^A=B} \mathrm{Det}[B] = e^{\mathrm{Tr}\{\ln(B)\}}. \tag{1.6}$$

[II]It could also be coupled to fermions. However, this will lead to the same result with a more complicated path, which will be disregarded. Scalar QCD could have also been an option. The fact that it lead to more diagrams was the reason for omitting this latter option.

In the present case

$$\mathrm{Det}[\sqrt{-g}] = e^{\frac{1}{2}\mathrm{Tr}\left\{\ln\left(\delta^{\mu}_{\nu}+\kappa h^{\mu}_{\nu}\right)\right\}}. \tag{1.7}$$

Finally, an expansion for the ln will give

$$\mathrm{Det}[\sqrt{-g}] = e^{\frac{1}{2}\sum_{n=1}^{\infty}\frac{(-\kappa)^n}{n}\mathrm{tr}(h^n)}, \tag{1.8}$$

which is already a relation between the determinant and powers of the graviton. The exponential expansion is trivial to do and will not be detailed here. The reader should already have guessed that the point is that one has infinite rules for QG. Each rule will increase in the number of gravitons. Moreover, each FR involves increasingly many terms, leading to an increase of the computation time. To give an example, the first FR only with gravitons, that is not the propagator, has 384 terms in a simple gauge. The complete set of FR used in this thesis is given in Appendix. B.

1.3.1 The (extreme) chaos of conventions

Let us revisit the differences between using κ, 2κ, or another conventions, as it has some noticeable consequences. The problem encountered has not been this simple rescaling, but rather something more subtle: a change in the definition of κ. The general notations are $\kappa^2 = 32\pi G_N$ ([16, 17, 18]), or $\kappa'^2 = 16\pi G_N$ ([12]). Going from one to another is trickier than it may seem, and it caused problems during the thesis. When the same powers of κ as $h_{\mu\nu}$ appear, this change can be absorbed[III]. This will happen everywhere except in the factor multiplying EH Lagrangian, where a factor of $1/\kappa^2$ is present. Thus it can be noticed that in some Lagrangians there is $-R/\kappa'^2$ instead of what has been stated in Eq. (1.4) . This will seem to affect the FR of the gravitons as well as the propagator. Let us analyze this in more detail.

All the terms of pure gravity will be multiplied by a factor of 2. Consequently the FR will be multiplied by the same factor. However, in the Lagrangian it always appear $2/\kappa^2$ or $1/\kappa'^2$ and both of these terms give $1/16\pi G_N$. Thus, what would seem a difference, in the end result should not affect physical results. The same will happen to the propagator, which will be multiplied by a factor of 2 when we have κ', by comparison to the case of κ[IV].

Finally, it is worth mentioning the role of combinatorial factors, which arise when vertices involve multiple gravitons as well as scalars. In the library of Mathematica used in this thesis ([19, 20, 21]), an extra factor of $1/2$ appears in the vertex with two scalars and two gravitons, as can be confirmed by direct comparison. Our interpretation is that this originates from treating gravitons as indistinguishable. Since one graviton is internal and the other external, there are two possible contractions, so the Feynman rule in the library effectively needs to be multiplied by 2. We emphasize that this is only a conjecture, as the point is not discussed in the references. Nonetheless, without this factor our consistency checks would fail, which strongly suggests that it must be included.

[III] To do this, one has $\kappa h_{\mu\nu} = (\kappa\cdot\sqrt{2})\cdot(h_{\mu\nu}/\sqrt{2}) = \kappa' h'_{\mu\nu}$, where $h'_{\mu\nu} = h_{\mu\nu}/\sqrt{2}$ and κ' has been already defined. Thus, when comparing the amplitudes with κ^n one would find a factor of $(2)^{n/2}$ that has been absorbed into the field definition.

[IV] All of this has a similar effect to the coupling in the final amplitude.

These have been among the main challenges encountered when computing the effective vertices in gravity. The intended take-home message is that conventions should always be checked carefully, even in seemingly subtle cases.

2 Introduction to High Energy scattering

Since the aim of this thesis is to test the double-copy in the so-called Regge regime, an introduction to the framework of high-energy scattering in QCD is now given.

It is well known that QCD can be treated perturbatively in the high-energy regime, where it does not confine. By analyzing an effective vertex and effective propagators in this regime one can obtain some lessons in quantum gravity through the double-copy structure introduced above. A close following of [22, 23, 24] has been made during this whole section. In addition, further papers will be cited where appropriate.

The following introduction might seem a slight digression, but it will be the basis to talk about the resummation process and is essential, since the process analyzed in this thesis ($qq' \to qq'g$) occurs inside hadrons. Later on, the result of this resummation, known as the reggeized gluon (and graviton correspondingly), will be discussed. Along some useful parametrization, the last part of this section will cover the so-called Regge limit.

2.1 Hadron scattering

It is an established result that the cross-section for the scattering of hadrons is approximated by

$$\sigma = \sum_{ab} \int_{\zeta_a}^{1} dx_a \int_{\zeta_b}^{1} dx_b f_{a/A}(x_a, \mu^2) f_{b/B}(x_b, \mu^2) \hat{\sigma}_{ab}(\zeta_a/x_a, \zeta_b/x_b, \alpha_s(\mu^2), Q^2/\mu^2), \tag{2.1}$$

where ζ_i is the minimum partonic momentum carried by particle i that is needed for the process to take place, $\hat{\sigma}_{ij}$ is the partonic cross section, x_i are the partonic momentum fraction, i.e., the momentum fraction that each parton carries with respect to the parent hadron, Q^2 is the hard scale of the process[V], μ^2 the renormalization scale, and $f_{j/J}(x_j, \mu^2)$ is the probability that the parton j is found inside the parent hadron J carrying momentum fraction x_j. The latter are usually called Parton Distribution Functions (PDFs). Universality of the PDFs is a well-known fact. This means that they do not depend on the specific process considered and are not computable using perturbation theory. This equation is only valid in the limit where $Q \to \infty$ and x is fixed. At finite values of Q an expansion in terms of $1/Q$ exists. In this expansion, one can see that Eq. (2.1) constitutes the leading term, called the leading twist. The other terms are called the higher twist. Since they do not play a role, they are ignored.

When computing the partonic cross section, two types of divergences arise, the ultraviolet (UV) and the infrared (IR). The UV divergences can be handled with a regularisation scheme which will introduce a non-physical scale μ^2. However, the IR is trickier, as there also appear two more types: soft and collinear divergences. After including the radiative corrections to a given

[V] The hard scale of some process is what defines the energy range at which this process can take place.

order one can solve the soft divergences. The interpretation of the collinear divergences is that they are the outcome of the collinear emission of partons. These are the processes such that an initial parton a with momentum fraction x_a emits a parton c during the hadron collision. This last parton, c, has momentum ζ_a and virtuality μ^2 [VI]. These collinear divergences are usually absorbed in the PDFs, which cancel the divergence upon renormalization. The renormalization group equations, i.e., the equations which state that physical quantities should be independent of the renormalization scale, in terms of the PDFs are written as

$$\frac{df_{a/A}(x,\mu^2)}{d\ln\mu^2} = \sum_c \int_x^1 \frac{d\xi}{\xi} P_{ac}\left(\xi, \alpha_s(\mu^2)\right) f_{c/A}\left(\frac{x}{\xi}, \mu^2\right). \tag{2.2}$$

These are the so-called Altarelli-Parisi, or DGLAP (Dokshitzer-Gribov-Lipatov-Altarelli-Parisi), evolution equations. P_{ac} are the well-known splitting functions, which can be obtained, using perturbation theory in QCD, as

$$P_{ac}(\xi, \alpha_s(\mu^2)) = \sum_{n=1}^{+\infty} \left(\frac{\alpha_s}{2\pi}\right)^n P_{ac}^{n-1}(\xi). \tag{2.3}$$

Eq. (2.2) reflects the collinear evolution previously mentioned. Also note that all computations assume massless particles, neglecting transverse momentum at this order. These corrections correspond to the higher-twist terms mentioned earlier.

2.2 Large rapidities

Once the analysis of the hadronic cross-section is done, the relevant energy regime needs to be identified. For example, in the Fermilab, it arises at a Center of Mass (CM) energy much larger than the hard scale, which is the so-called semi-hard regime. At large energies[VII] it is known that $\sqrt{s} = \sqrt{x_a x_b \hat{s}}$ where $\hat{s}$ is the Mandelstam variable of the partons. Then, one can make the decomposition

$$\ln\left(\frac{s}{Q^2}\right) = \ln\left(\frac{1}{x_A}\right) + \ln\left(\frac{\hat{s}}{Q^2}\right) + \ln\left(\frac{1}{x_B}\right). \tag{2.4}$$

It is known that $\ln(1/x)$ appears in the DGLAP evolutions (Eq. (2.2)) while $\ln\left(\hat{s}/Q^2\right)$ parametrizes the hard scattering. In the semihard regime, the left-hand side of Eq. (2.4) becomes large either due to a large $\ln(1/x)$ or a large $\ln\left(\hat{s}/Q^2\right)$. Under the consideration that $\ln(1/x)$ is small, i.e., x is of order unit, the large contribution comes from $\ln\left(\hat{s}/Q^2\right)$. However, $\ln\left(\hat{s}/Q^2\right)$ appear in different diagrams, and thus, the sum over all of these diagrams will be considered. This sum is known as the resummation process. The first resummation techniques developed were implemented in the high-energy limit of QED. The leading contribution to this theory can be shown to come from the t-channel in the high-energy limit. This theory has some radiative corrections that indicate that one needs to resum over $\alpha^2 \ln\left(\hat{s}/Q^2\right)$ (which is of order unit). Despite the fact that in QCD it can also be shown that the leading contribution also comes from the t-channel[VIII], the resummation in this theory needs to be done over $\alpha_s \ln\left(\hat{s}/Q^2\right)$ (which will

[VI] The virtuality describes how far this parton is from being on-shell.

[VII] If the particles are massless, or if the energy is much higher than the mass.

[VIII] This only happens in the physical gauges. A physical gauge is somewhat more difficult to define. It is not as simple as choosing the R_ξ gauges that are more common to work with, but a gauge such that no ghosts particle can be found [25, 26]. For the purposes of this thesis, the specific gauge choice will not matter, as the t-channel dominates in all cases considered.

be of order unit now). Diagrams with different orders than this, for example, $\alpha_n^2 \ln(\hat{s}/Q^2)$ are known as the next order. Staying with the same powers of α_n and $\ln(\hat{s}/Q^2)$ is known as the logarithmic leading order (or sometimes referred to LLO, and the next order will be the NLLO). The fact that one can neglect the other channels in these gauges at large energies justifies that one can deal with only the t-channel without caring about the quarks. For example, in the process $q\overline{q} \to q\overline{q}g$, being q a quark and $\overline{q}$ its antiparticle, the s-channel should be considered. Motivated by this, one can work with the more general $qq' \to qq'g$ where q and q' are random quarks.

2.3 Reggeized gluon

The resummation discussed above can be performed at the level of amplitudes. It can be shown that the process

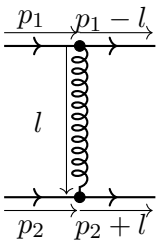

has an amplitude $M^0_{qq\to qq}(\vec{l}_\perp)$. Its functional form will not matter for the discussion done in this thesis. Analyzing the one-loop processes, which involves all the diagrams that only have 2 gluons, for example

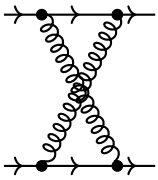
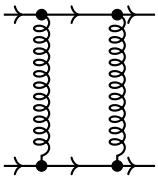

the effect of the resummation can be seen. Diagrams including fermions in the loop as well as gluons in closed loops, such as

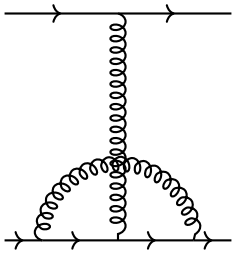

are excluded. It can be shown that such diagrams contribute at NLLO as they come with $\alpha_n^2 \ln(\hat{s}/Q^2)$ [27]. This can be easily seen by the fact that when computing the bubble sub-diagram, it will not give any contribution proportional to s, and thus no extra power in the logarithm will appear. The same argument can be applied to the loops with quarks ([28]). In the latter case, the quarks always appear with their antiquark pair, which will be closed in a

bubble diagram. Computing the one-loop correction yields

$$M^1_{qq\to qq}(\vec{l}_\perp) = M^0_{qq\to qq}(\vec{l}_\perp)\omega(\vec{l}_\perp)Y, \tag{2.5}$$

where

$$\omega(\vec{l}_\perp) = \frac{-\alpha_s N_c}{4\pi^2}\int d^2q_\perp \frac{\vec{l}_\perp^{\,2}}{\vec{q}_\perp^{\,2}(\vec{q}_\perp - \vec{l}_\perp)^2}, \tag{2.6}$$

and $Y = \ln(s/k_\perp^2)$. $\omega(\vec{l}_\perp)$ is called the Regge trajectory of the gluon. We refer to [23] for a more detailed computation. As it is a result already done, and not the focus of this thesis, the computations are omitted. By doing the same for all the loop contributions, one gets

$$M_{qq\to qq} = M^0_{qq\to qq}e^{\omega(\vec{l}_\perp)Y}. \tag{2.7}$$

This can be interpreted as a change of the gluon propagator. If the gluon propagator is $A_{\mu\nu}(\xi, l)$, which depends on the gauge (ξ) and its momentum (l), when considering all the diagrams, one gets the following effective propagator

$$A_{\mu\nu}(\xi, l) \to A_{\mu\nu}e^{\omega(\vec{l}_\perp)Y}, \tag{2.8}$$

This is interpreted as an effective gluon, known as the Reggeized gluon. Diagrammatically, this is seen as

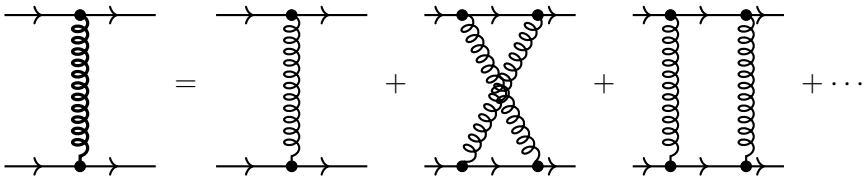

In different articles ([24]), these corrections are also known as virtual radiative corrections, while in some others, this is known as the Reggeized gluon ([23]).

This regime can also be addressed within the framework of effective field theory ([29, 30]). While a detailed discussion is beyond the scope of this thesis, it is worth noting that the approach adopted here is not unique.

2.4 Reggeized graviton

The case of the graviton is not so simple. The amplitude can be computed to be ([31, 32])

$$A_{4,(\mathcal{N})} = A_4\mathcal{M}_{4,(\mathcal{N})}, \tag{2.9}$$

where A_4 is the tree-level amplitude, $\mathcal{N}$ are the number of gravitinos and $\mathcal{M}_{4,(\mathcal{N})}$ has the loop corrections. One finds that

$$\mathcal{M}_{4,(\mathcal{N})} = 1 + \sum_{L=1}^{\infty}\mathcal{M}^{(L)}_{4,(\mathcal{N})}, \tag{2.10}$$

where L are the number of loops. At one-loop and $\mathcal{N}=8$, one finds ([31, 32])

$$\mathcal{M}^{(1)}_{4,(\mathcal{N}=8)} = \underbrace{\alpha t \ln\left(\frac{s}{t}\right)\ln\left(\frac{u}{t}\right)}_{\text{Double logs}} + \underbrace{\alpha\frac{t}{2}\ln\left(\frac{-t}{\lambda^2}\right)\left(\ln\left(\frac{s}{t}\right)+\ln\left(\frac{s}{t}\right)\right)}_{\text{Trajectory}}$$
$$\underbrace{-\alpha\frac{s-u}{2}\ln\left(\frac{-t}{\lambda^2}\right)\ln\left(\frac{s}{u}\right)}_{\text{Eikonal}}. \tag{2.11}$$

This complication gives rise to the difficulties in the computation of the Reggeized graviton. Additional terms must be analyzed to determine the dominance. As a matter of fact, in the Regge limit, which will be carefully analyzed in the next subsection, what dominates is not the trajectory, but the Eikonal component.

Not only is the task of resumming this laborious, but also is a state-of-the-art topic. Motivated by this, the focus of this work will be the trajectory, while ignoring the eikonal and the double logarithms. The results can be found in [31, 32, 33, 34]. The Regge trajectory for the graviton is given by

$$\omega(q^2) = q^2\frac{\kappa^2}{(2\pi)^3}\int\frac{d^2k_\perp}{k_\perp^2(q-k_\perp)^2}\{(k_\perp,q-k_\perp)^2(k_\perp^{-2}+(q-k_\perp)^{-2})-q^2-\frac{N}{2}(k_\perp,k_\perp-q)\}, \tag{2.12}$$

where N is the number of gravitinos in the N-extended SUSY.

2.5 The multi-parton and Regge Kinematics

Amplitudes of two partons going to $n+2$ partons are considered for the remainder of the section. In particular, as shown in Fig. 1, this thesis focuses on the scenario of two quarks going into n gluons and two quarks.

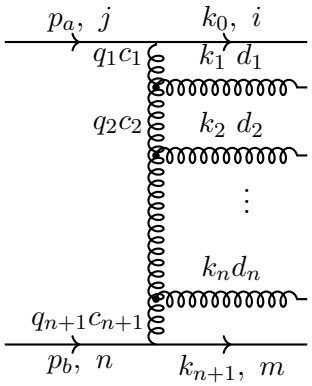

Figure 1: Multi-gluon exchange ladder diagram

One can label the momenta of outgoing partons as

$$k_i = (k_{i\perp}e^{y_i}, k_{i\perp}e^{-y_i}, \vec{k}_{i\perp}), \tag{2.13}$$

where y_i are the rapidities, and $i = 0, \ldots, n+1$. The ingoing particles have momenta

$$\begin{cases} p_a = (\sqrt{s}x_A, 0, \vec{0}); \\ p_b = (0, \sqrt{s}x_B, \vec{0}). \end{cases} \tag{2.14}$$

In the CM, $x_A = x_B = 1$. Then, the conservation equations can be written as

$$\begin{aligned} \vec{0} &= \sum_{i=0}^{n+1} \vec{k}_{i\perp}; \\ (1 =) x_A &= \sum_{i=0}^{n+1} \frac{k_{i\perp}}{\sqrt{s}} e^{y_i}; \\ (1 =) x_B &= \sum_{i=0}^{n+1} \frac{k_{i\perp}}{\sqrt{s}} e^{-y_i}. \end{aligned} \tag{2.15}$$

A generalization of the Mandelstam variables is given by

$$\begin{aligned} \hat{s} &= x_A x_B s = \sum_{i,j=0}^{n+1} k_{i\perp} k_{j\perp} e^{y_i - y_j}; \\ \hat{s}_{ai} &= -2 p_a k_i = -\sum_{j=0}^{n+1} k_{i\perp} k_{j\perp} e^{-(y_i - y_j)}; \\ \hat{s}_{bi} &= -2 p_b k_i = -\sum_{j=0}^{n+1} k_{i\perp} k_{j\perp} e^{(y_i - y_j)}; \\ \hat{s}_{ij} &= 2 k_i k_j = 2 k_{i\perp} k_{j\perp} (\cosh(y_i - y_j) - \cosh(\phi_i - \phi_j)), \end{aligned} \tag{2.16}$$

where it has been assumed that all particles are massless, or that the energy is big enough to neglect the masses. ϕ_i are the angles of the perpendicular direction. Once this is defined, one can introduce the Multi-Regge Kinematics limit. The main idea of this limit is to have an ordering in terms of the momenta of the outgoing particles. Formulated with rapidities, the MRK condition can then be expressed as

$$y_0 >> y_1 >> \cdots >> y_{n+1}; \qquad k_{i\perp} \sim k_\perp. \tag{2.17}$$

Other classifications in terms of the so-called light-cones variables are present in the literature ([35]). These variables are defined through

$$k_i^\pm = k_i^0 \pm k_i^3. \tag{2.18}$$

In this parametrization, the metric, or the product of four-vectors, is given by

$$q \cdot p = \frac{1}{2}(q_+ p_- + p_+ q_-) - \vec{q}_\perp \vec{p}_\perp \tag{2.19}$$

Then, the rapidity is given by

$$y_i = \ln\left(\frac{k_i^+}{k_i^-}\right). \tag{2.20}$$

The MRK limit can now be interpreted as

$$k_0^+ >> \cdots >> k_{n+1}^+; \qquad k_0^- << \ldots k_{n+1}^-. \tag{2.21}$$

These two conditions are accompanied by having a similar transverse momentum, i.e., $k_{0,\perp} \sim \cdots \sim k_{n+1,\perp}$. As stated in [22] one can parameterize the light cone variables in terms of a small parameter ϵ by using that each $>>$ goes with a factor of ϵ. With this in mind, it can be found

$$k_j^+ = \mathcal{O}\left(\epsilon^{-\frac{n-1}{2}+j}\right); \qquad k_j^- = \mathcal{O}\left(\epsilon^{\frac{n-1}{2}-j}\right). \tag{2.22}$$

This also comes from choosing how p_0^+ scales with ϵ. It is common to choose that $\mathcal{O}(p_0^+) = \mathcal{O}(1/p_{n+1}^+)$. Moreover, in this limit the Mandelstam variables also follow an order. Let us look at an example of five particles and compare it to the case discussed in [12]. For each momentum, an introduction of two energy scales $\Lambda_j^{\pm}$ is also necessary. These energy scales follow that $\Lambda_i \sim \Lambda_j$ $\forall i,j$ and $\Lambda_i^+ \sim \Lambda_i^-$ $\forall i$. Thus, one is able to write

$$\begin{cases} k_0 = (\epsilon^{-1}\Lambda_0^+, \epsilon\Lambda_0^-, k_{0,\perp}); \\ \\ k_1 = (\epsilon^0\Lambda_1^+, \epsilon^0\Lambda_1^-, k_{1,\perp}); \\ \\ k_2 = (\epsilon^1\Lambda_2^+, \epsilon^{-1}\Lambda_2^-, k_{2,\perp}). \end{cases} \tag{2.23}$$

Notice that not only are the scales $\Lambda^{\pm}$ related to $k_\perp$ but also we have that ϵ is somehow related to $e^{y_{\text{IX}}}$. Without further detail, this can be seen by looking at Eq. (2.13). Furthermore, the conservation equations are now written as

$$\begin{cases} \sqrt{s} = \epsilon^{-1}\Lambda_0^+ + \Lambda_1^+ + \epsilon\Lambda_2^+; \\ \\ \sqrt{s} = \epsilon\Lambda_0^- + \Lambda_1^- + \epsilon^{-1}\Lambda_2^-; \\ \\ 0 = k_{0,\perp} + k_{1,\perp} + k_{2,\perp}. \end{cases} \tag{2.24}$$

At leading order, it can be seen that $\Lambda \propto \sqrt{s}\epsilon^{-1}$. A more general result leads to $\Lambda \propto \sqrt{s}\epsilon^{-\frac{n+1}{2}}$. Through the definition (Eq. (2.16)) one can obtain

$$\begin{cases} \hat{s}_{a0} = -\Lambda_0^+\sqrt{s}\epsilon; \qquad \hat{s}_{b2} = -\Lambda_2^-\sqrt{s}\epsilon; \\ \\ \hat{s}_{a1} = \Lambda_1^+\sqrt{s}; \qquad \hat{s}_{b1} = \Lambda_1^-\sqrt{s}. \end{cases} \tag{2.25}$$

With this, under the assumption that $\sqrt{s} >> \Lambda_i$ $\forall i$ one gets

$$s >> \hat{s}_{b1} \sim \hat{s}_{a1} >> \hat{s}_{a0} \sim \hat{s}_{b2}. \tag{2.26}$$

[IX] We could relate $\Lambda_i \propto |k_{i,\perp}|$ and $\epsilon^2 \propto e^{-y_0}$.

Which agrees with the relation stated in [12].

2.6 Sudakov parametrization

It is very common and useful to work with the so-called Sudakov parametrization. In this parametrization, the amplitudes under consideration simplify greatly ([12]). In terms of Fig. 1, the transverse momenta will be written as

$$q_n^\mu = \alpha_n p_a^\mu + \beta_n p_b^\mu + q_{n,\perp}^\mu. \tag{2.27}$$

For example, it is known that $q_1^\mu = p_a^\mu - k_0^\mu$, and thus,

$$q_1 \cdot p_a = \frac{\hat{s}}{2}\beta_1 = k_0 \cdot p_a = \hat{s}_{a0}/2 \rightarrow \beta_1 = \frac{\hat{s}_{a0}}{\hat{s}}. \tag{2.28}$$

In general, one finds

$$q_n = q_{n-1} - k_{n-1} = p_a - \sum_{i=0}^{n-1} k_i. \tag{2.29}$$

As an example, consider the process $qq \rightarrow qqg$. In such a case, one can see that $q_2^\mu = k_2^\mu - p_b^\mu$ and $k_1^\mu = q_1^\mu - q_2^\mu$. From

$$q_2^\mu = \alpha_2 p_a^\mu + \beta_2 p_b^\mu + q_{2,\perp}^\mu \tag{2.30}$$

one obtains

$$\begin{cases} k_0 = (1-\alpha_1)p_a^\mu - \beta_1 p_b^\mu - q_{1,\perp}^\mu; \\ k_1 = (\alpha_1 - \alpha_2)p_a^\mu + (\beta_1 - \beta_2)p_b^\mu + (q_{1,\perp}^\mu - q_{2,\perp}^\mu); \\ k_2 = \alpha_2 p_a^\mu + (1+\beta_2)p_b^\mu + q_{2,\perp}^\mu. \end{cases} \tag{2.31}$$

Then it follows

$$q_1 \cdot p_b = \frac{\hat{s}}{2}\alpha_1 = (p_a - k_0)\cdot p_b = \frac{\hat{s}}{2} - \frac{\hat{s}_{b0}}{2} = \frac{\hat{s}}{2} - \frac{\sqrt{\hat{s}}}{2}\epsilon^{-1}\Lambda_0^+. \tag{2.32}$$

Using Eq. (2.24), one reaches

$$\alpha_1 \hat{s} = \sqrt{\hat{s}}(\Lambda_1^+ + \epsilon\Lambda_2^+) \approx \sqrt{\hat{s}}\Lambda_1^+ \rightarrow \alpha_1 \approx \frac{\Lambda_1^+}{\sqrt{\hat{s}}} << 1. \tag{2.33}$$

Proceeding in this way, the following relation can be easily proved

$$1 >> \alpha_1 \sim \beta_2 >> \alpha_2 \sim \beta_1, \tag{2.34}$$

which is the MRK limit in terms of the Sudakov parameters. Furthermore, one can also obtain the relations

$$\hat{s}_{01} = -\hat{s}(\alpha_2 + \beta_2); \qquad \hat{s}_{21} = \hat{s}(\alpha_1 + \beta_1); \qquad \hat{s}_{a0} = -t = -\hat{s}\beta_1;$$

$$\hat{s}_{b2} = -t' = \hat{s}\alpha_2; \qquad \hat{s}_{a1} = \hat{s}(\beta_1 - \beta_2); \qquad \hat{s}_{b1} = \hat{s}(\alpha_1 - \alpha_2); \tag{2.35}$$

$$\hat{s}_{a2} = \hat{s}(1 + \beta_2); \qquad \hat{s}_{b0} = \hat{s}(1 - \alpha_1); \qquad \hat{s}_{02} = \hat{s}(1 - \alpha_1 + \alpha_2 - \beta_1 + \beta_2).$$

All of these relations will be useful and will appear in the calculations that will be performed later. These relations are therefore essential for the subsequent calculations.

2.7 Eikonal approximation

In addition, the Regge limit also introduces the so-called *eikonal approximation*. In this approximation, the momentum carried by the emitted gluons is considered to be negligible compared to the quarks (both the incoming and the outgoing ones). This can already be seen in Eq. (2.23), where the components of the quarks that dominate go as ϵ^{-1} while all the components of the gluon go as ϵ^0. The same happens with q_1 and q_2. Thus, the approximation consists in taking

$$\begin{cases} k_0 = p_a - q_1 \approx p_a; \\ \\ k_2 = p_b + q_2 \approx p_b. \end{cases} \tag{2.36}$$

Expressions similar to $k_2 - p_b + k_1$ will have to be treated with more care. In these cases, as k_1 and q_2 are of the same order, one cannot neglect the q_2 term coming from $k_2 - p_b$ and thus $k_2 - p_b + k_1 = q_2 + k_1$. Also, terms such as $\alpha_1 p_1 + q_{1,\perp}$ cannot be straightforwardly approximated. As it has already been stated that $\Lambda \propto \epsilon$ and one knows that Λ and $k_\perp$ are related, we can see that $k_\perp \propto \epsilon$. Thus, terms like $\alpha_1 p_1 + q_{1,\perp}$ cannot be approximated.

3 Procedure

The computations presented here were performed using three Mathematica libraries: FeynCalc (FC) ([36, 37, 38, 39]), FeynArts (FA) ([40]), and FeynGrav (FG) ([19, 20, 21]).
Before proceeding, it is useful to briefly explain why multiple libraries are needed and what their respective roles are.

Historically, FA was developed first, with the primary purpose of generating Feynman diagrams for various processes according to the standard FR. FC, developed later, serves a different role: it provides tools for carrying out algebraic computations of the quantities appearing in amplitudes, such as spinor chains, tensor contractions, and loop integrals. FC was designed to be compatible with FA—one can generate diagrams with FA and then evaluate them with FC. The most recent development is FG, which enables similar computations to FC but implements the FR of QG.

For FA to work, it requires a model file containing the FR and particle spectrum for the theory under consideration. In the case of perturbative QCD, these are already included in FA by default. However, the situation is different for perturbative QG: its FR are less common and therefore not built into FA. Although FG contains the FR for QG, they are implemented in a way that is incompatible with FA. Consequently, FG is best viewed as an extension of FC, not FA, meaning that the workflow for computing amplitudes in QCD and in QG must be handled differently. Specifically, when working with QG, the diagrams must first be drawn manually, and all relevant FR—propagators, vertices, and so on—must then be entered by hand.

For a more detailed introduction to these libraries, see Sect. C, where examples in QED, QCD and QG, along with explanations of how the corresponding code operates are provided.

In what follows, the process of gluon radiation from the interaction of two distinguishable quarks is presented for the QCD scenario, which is typically known as a five-point amplitudes (in general, amplitudes with n external particles are known as n-point amplitudes). By applying the MRK limit to this amplitude, an effective vertex between gluons will be derived. The first step will consist of a discussion about the effective vertex in QCD while the explanation of how to implement the steps in the code is given simultaneously[X]. The procedure is repeated in the QG context using scalars and gravitons instead of quarks and gluons, respectively. In this second case, the effective vertex will involve gravitons instead of gluons. In the next section a discussion of the results obtained here will be made, in addition to the comparison between the QCD and the QG effective vertices.

All code presented in this thesis was written by the author. While the underlying computations have been performed before, they were carried out in a more cumbersome way; the present implementation streamlines the process, enabling easier extension to, for example, the computation of the six-point amplitude (see Sect. 6.2).

3.1 QCD effective vertex in the Regge limit

The process of $qq' \to qq'g$ has the diagrams shown in Fig. 1

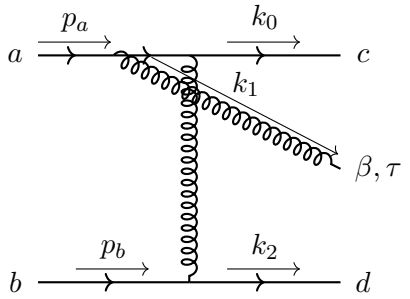

(a) Diagram where the upper quark has an initial bremsstrahlung.

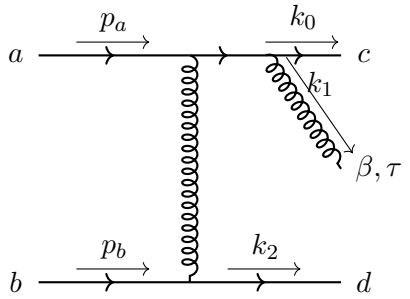

(b) Diagram where the upper quark has a final bremsstrahlung.

[X]Some auxiliary functions—unrelated to the core physics—were implemented to handle relabeling or intermediate program-specific issues. These are not discussed here but can be found, with the whole code, at https://github.com/P3p2002/Double-copy-structure-From-QCD-to-gravity

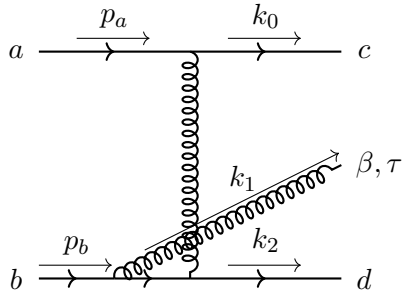

(e) Diagram where the lower quark has an initial bremsstrahlung.

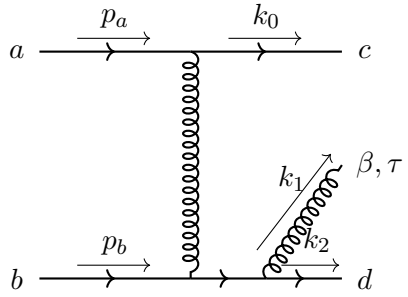

(f) Diagram where the lower quark has a final bremsstrahlung.

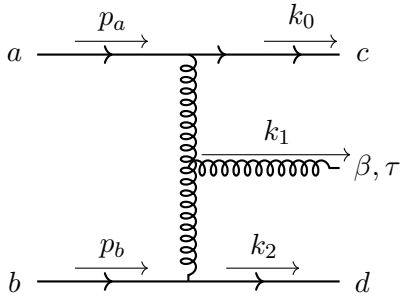

(g) Diagram where we find the emission of a gluon in the virtual gluon exchange.

Figure 1: All of the possible diagrams for the process of $qq' \to qq'g$. The corresponding amplitudes will be labeled as M_i with $i = 1, ..., 5$.

The corresponding amplitudes are given in Eqs. (3.1)

$$
\begin{aligned}
M_1 &= \frac{g_s^3 T^\alpha_{db}(T^\alpha T^\beta)_{ca}}{s_{a1}t'}\overline{u}(k_2)\gamma^\mu u(p_b)\overline{u}(k_0)\gamma_\mu(\not{p}_a - \not{k}_1)\not{\epsilon}(k_1)u(p_a);\\
M_2 &= -\frac{g_s^3 T^\alpha_{db}(T^\beta T^\alpha)_{ca}}{s_{01}t'}\overline{u}(k_2)\gamma^\mu u(p_b)\overline{u}(k_0)\not{\epsilon}(k_1)(\not{k}_0 + \not{k}_1)\gamma^\mu(p_a);\\
M_3 &= -\frac{g_s^3 T^\alpha_{ca}(T^\alpha T^\beta)_{db}}{s_{a0}s_{b1}}\overline{u}(k_0)\gamma^\mu u(p_a)\overline{u}(k_2)\gamma_\mu(\not{p}_b - \not{k}_1)\not{\epsilon}(k_1)u(p_b);\\
M_4 &= \frac{g_s^3 T^\alpha_{ca}(T^\beta T^\alpha)_{db}}{s_{a0}s_{12}}\overline{u}(k_0)\gamma^\mu u(p_a)\overline{u}(k_2)\not{\epsilon}(k_1)(\not{k}_1 + \not{k}_2)\gamma_\mu(p_b);\\
M_5 &= -\frac{ig_s^3 T^\gamma_{ca}T^\alpha f^{\beta\gamma\alpha}}{t's_{a0}}\overline{u}(k_1)\gamma_\mu u(p_a)\overline{u}(k_2)\gamma_\nu u(p_b)[2(p_b - k_2)\cdot\epsilon(k_1)\eta^{\mu\nu} +\\
&(2k_1 + k_2 - p_b)^\nu\epsilon^\mu(k_1) + \epsilon^\nu(k_1)(k_2 - k_1 - p_b)^\mu]
\end{aligned}
\tag{3.1}
$$

Once the amplitudes are computed, one can separate them into two gauge invariant sectors ([12]). This will be useful for simplifying the computations, especially for the spinorial structures. These sectors are given by

$$
M_\uparrow = M_1 + M_2 + \frac{t}{t - t'}M_5; \qquad M_\downarrow = M_3 + M_4 - \frac{t}{t - t'}M_5. \tag{3.2}
$$

They can be shown to be gauge invariant by verifying the Ward identities, i.e.,

$$
k_{1\mu}M^\mu_\uparrow = 0; \qquad k_{1\mu}M^\mu_\downarrow = 0. \tag{3.3}
$$

One can define

$$M_{\uparrow} = \epsilon^{\tau}(k_1)\overline{u}(k_0)\Lambda^{\chi\tau}_{ca;\alpha\beta}u(p_a)\overline{u}(k_2)T^{\alpha}_{db}g_s\gamma^{\chi}u(p_b); \tag{3.4}$$

$$M_{\downarrow} = \epsilon^{\tau}(k_1)\overline{u}(k_0)T^{\alpha}_{ca}g_s\gamma^{\chi}u(p_a)\overline{u}(k_2)\Lambda^{\chi\tau}_{db;\alpha\beta}u(p_b), \tag{3.5}$$

which will be interpreted as effective vertices for the two sectors defined before. Diagrammatically, this is represented as

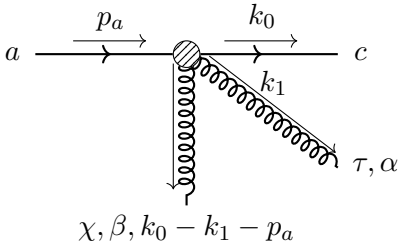

$$= \qquad \Lambda^{\chi\tau}_{ca;\alpha\beta}.$$

The functional form of $\Lambda^{\chi\tau}_{ca;\alpha\beta}$ will be seen once the proper calculations are done. Note that the gluon with index χ is off-shell, while all the other particles are on-shell. The procedure to arrive at Eq. (3.1) only involved simple functions of FC and FA as well as using the Sudakov parametrization. It is from this point where the coding starts to get tricky. By looking at the code, the result of $M_{\uparrow}$ was far from Eq. (3.4). To avoid giving the whole result, which is too lengthy, a simpler example will be given to understand what was wrong with the output. The subamplitude of Mathematica was given by

$$M = \epsilon^{\lambda}\overline{u}(k_2)\gamma_{\rho}u(p_b)\overline{u}(k_1)\not{q}\gamma^{\rho}\gamma_{\lambda}u(p_a) + \epsilon^{\tau}\overline{u}(k_2)\gamma_{\mu}u(p_b)\overline{u}(k_1)\gamma_{\tau}\gamma^{\mu}\not{q}u(p_a).$$

This can be simplified by relabeling dummy indices and factoring out the polarization. A comparison with Eq. (3.4) will be possible once the proper functions that simplify the example given are made. To solve the problem about relabeling and factoring out the polarization, the function `FactorOutPolarizations[expr_, lorentzIndex_: \[Tau]]` was created. Once it is applied to the given example, one obtains

$$M = \epsilon^{\tau}(\overline{u}(k_2)\gamma_{\rho}u(p_b)\overline{u}(k_1)\not{q}\gamma^{\rho}\gamma_{\tau}u(p_a) + \overline{u}(k_2)\gamma_{\mu}u(p_b)\overline{u}(k_1)\gamma_{\tau}\gamma^{\mu}\not{q}u(p_a)).$$

The next step is to collect the spinor structures. A relabeling of the gamma matrices indices will help in such process. The function `ReplaceGammaIndicesInSpinorChain[expr_, {kin_, pin_}, dummyIndex_]` changes the dummy index of the gamma matrix as

$$\overline{u}(kin)\gamma^{\tau}u(pin) \to \overline{u}(kin)\gamma^{\chi}u(pin)\delta^{\tau}_{\chi}, \tag{3.6}$$

where the dummyIndex has been χ. In the given example one should use `ReplaceGammaIndicesInSpinorChain [Ex, {k2, pb}, \ [Chi]]` to obtain

$$M = \epsilon^{\tau}\overline{u}(k_2)\gamma_{\chi}u(p_b)(\overline{u}(k_1)\not{q}\gamma^{\chi}\gamma_{\tau}u(p_a) + \overline{u}(k_1)\gamma_{\tau}\gamma^{\chi}\not{q}u(p_a)).$$

A factorization of the spinors that enclose what will be our $\Lambda^{\chi\tau}_{ca;\alpha\beta}$ matrix will follow. This is done through the function `FactorSpinorChain[expr_, k_, p_]`. By applying `FactorSpinorChain[M,`

`k_1, p_a]` one obtains

$$M = \epsilon^{\tau}\overline{u}(k_2)\gamma_{\chi}u(p_b)\overline{u}(k_1)(\not{q}\gamma^{\chi}\gamma_{\tau} + \gamma_{\tau}\gamma^{\chi}\not{q})u(p_a).$$

This already resembles Eq. (3.4). By applying these three functions to the $M_{\uparrow}$ in the code, one obtains

$$M_{\uparrow} = \frac{g_s^3\epsilon^{\tau}(k_1)T^{\alpha}_{db}}{t'}\overline{u}(k_2)\gamma^{\chi}u(p_b)\overline{u}(k_0)\Big[-\frac{\gamma^{\tau}(\not{k}_0+\not{k}_1)\gamma^{\chi}(T^{\beta}T^{\alpha})_{ca}}{s_{01}} + \frac{\gamma^{\chi}(\not{p}_a-\not{k}_1)\gamma^{\tau}(T^{\alpha}T^{\beta})_{ca}}{s_{a1}} - \frac{if^{\alpha\beta\gamma}T^{\gamma}_{ca}(2\gamma^{\chi}(k_2-p_b)^{\tau}-\gamma^{\tau}(2k_1+k_2-p_b)^{\tau}-(\not{k}_2-\not{k}_1-\not{p}_b)\eta^{\tau\chi})}{t-t'}\Big]u(p_a). \tag{3.7}$$

Comparing with Eq.(3.4) one obtains the functional form

$$\Lambda^{\tau\chi}_{ca;\alpha\beta} = \frac{g_s^2}{t'}\Big[-\frac{\gamma^{\tau}(\not{k}_0+\not{k}_1)\gamma^{\chi}(T^{\beta}T^{\alpha})_{ca}}{s_{01}} + \frac{\gamma^{\chi}(\not{p}_a-\not{k}_1)\gamma^{\tau}(T^{\alpha}T^{\beta})_{ca}}{s_{a1}} - \frac{if^{\alpha\beta\gamma}T^{\gamma}_{ca}(2\gamma^{\chi}(k_2-p_b)^{\tau}-\gamma^{\tau}(2k_1+k_2-p_b)^{\tau}-(\not{k}_2-\not{k}_1-\not{p}_b)\eta^{\tau\chi})}{t-t'}\Big]. \tag{3.8}$$

Working with Eq. (3.8) instead of the whole amplitude (Eq. (3.7)) will prove to be useful. This procedure greatly simplifies the coding.

Three functions have been defined to go from the full amplitude to the effective vertex. The first one is `removePolarization[expr_, mom_, lor_]`. This function removes the polarization, with the specified momentum and index, from the expression. The next function is `removeFermionBilinear [expr_, momL_, momR_, mu_]`, which will enable one to remove $\overline{u}(k_2)\gamma^{\chi}u(p_b)$ from Eq. (3.7). Finally `removeOuterSpinors[expr_, momL_, momR_]` does something similar by removing the spinors enclosing the effective vertex. Following this procedure, a function proportional to the effective vertex is obtained[XI]. Despite having removed all the spinors, one needs to remember that they are there. This procedure is used as a simplification of the coding part, it is not a physical simplification.

Until now, the effective vertex involves quarks, while it was stated that it should not. To obtain the double copy structure, one needs something only involving gluons. To get to this point, the eikonal approximation will prove its usefulness.

By means of the eikonal approximation, at leading order one finds

$$u(k_0) = u(p_a - q_1) \approx u(p_a); \qquad u(k_2) = u(p_b + q_2) \approx u(p_b). \tag{3.9}$$

The elimination of spinorial structures will be achieved using this together with the so-called Gordon decomposition. Using the equations of motion in addition to the normalization of the spinors([41])

$$\overline{u}(p)_a u(p)_b = 2m\delta_{ab},$$

one can obtain

$$\overline{u}(p)\gamma^{\mu}u(p) = 2p^{\mu}. \tag{3.10}$$

[XI] These coefficients are not crucial, since they can be removed more easily.

The short proof is left to the reader. This will be of much use, since Eq. (3.7) has precisely this kind of structures. In addition to these structures, Eq. (3.7) also has terms similar to

$$u(k_0)\gamma^\chi\gamma^\rho\gamma^\tau u(p_a)(p_a-k_1)_\rho. \tag{3.11}$$

The eikonal approximation now tells us that $k_0+k_1\approx p_a$ while $p_a-k_1\approx p_a$, which are the terms that appear in the amplitude. By also applying the eikonal approximation in the spinors (Eq. (3.9)), one obtains

$$\overline{u}(k_0)\gamma^\chi\gamma^\rho\gamma^\tau u(p_a)(p_a-k_1)_\rho\approx\overline{u}(p_a)\gamma^\chi\gamma^\rho\gamma^\tau u(p_a)(p_a)_\rho. \tag{3.12}$$

The equations of motion yield

$$\overline{u}(p_a)\gamma^\chi\gamma^\rho\gamma^\tau u(p_a)(p_a)_\rho=\overline{u}(p_a)(-\gamma^\rho\gamma^\chi+2\eta^{\chi\rho})\gamma^\tau u(p_a)(p_a)_\rho=2(p_a)^\chi\overline{u}(p_a)\gamma^\tau u(p_a). \tag{3.13}$$

Using Eq. (3.10) results in

$$\overline{u}(k_0)\gamma^\chi\gamma^\rho\gamma^\tau u(p_a)(p_a-k_1)_\rho\approx 4p^\chi p^\tau. \tag{3.14}$$

The necessary tools to handle the spinorial structures have now been presented (Eqs. (3.10) and (3.14)). The implementation of this into the code is nontrivial. The eikonal approximation works by just making the substitutions shown in Eq. (3.15).

$$k_0=p_a-q_1;\qquad k_1=q_1-q_2;\qquad k_2=p_b+q_2. \tag{3.15}$$

This is followed by the implementation

$$p_a+c\cdot q_i\approx p_a;\qquad p_b+b\cdot q_i\approx p_b, \tag{3.16}$$

where c and b are two constants of order 1, while $i=1,2$. All of this is implemented in the function `EikonalApprox[expr_]`.

The implementation of Eq. (3.14) has been done through `replaceInList[list_List, p_]`. The function will first search for a gamma matrix in the given expression. If found, it will search for another gamma matrix in a further position. This second gamma matrix will need to be contracted with the momenta `p`. Finally, it will search for the third gamma matrix. It will save the indices from the first and third gamma matrix, to use Eq. (3.14). This can be done as the spinors have been previously factored out. The last function is `GordonDecom[expr_, p_]`, which applies Eq. (3.10). The idea is just to make the substitution $\gamma^\mu\to 2p^\mu$ for whatever Lorentz index (μ) it has. It is important to know that the order of the functions matters now. The `EikonalApprox [expr_]` is the function that first needs to be applied. Then it will come `replaceInList`, which will approximate the terms with 3 gamma functions. Only once this is done, `GordonDecom` can be applied. For example, if the second function was `GordonDecom` all the terms with 3 gamma matrices will be wrongly substituted to $8p^\chi p^\rho p^\tau$. Also, if `EikonalApprox[expr_]` is not the first function, some momenta will not be approximated, and may cause some error.

After this is done, Eq. (2.35) can be applied to leave the result in terms of the Sudakov variables.

Moreover it will be important to keep in mind that $p_i \cdot q_{j,\perp} = 0$, where $i = a, b$ and $j = 1, 2$. Once this is done, for the effective vertex of $M_\uparrow$ one obtains

$$\Lambda^{\tau\chi}_{ca;\alpha\beta} \approx g_s^2 \frac{iT^\gamma_{ca} f^{\alpha\beta\gamma}}{\alpha_2 s^2(\alpha_2+\beta_1)}[(\beta_1-2\beta_2)\eta^{\tau\chi} + p_a^\chi(2(q_1+q_2)^\tau_\perp + 2(\beta_2+\beta_1)p_b^\tau + (4-2\alpha_1)p_a^\tau) \tag{3.17}$$

$$+ p_a^\tau(-4q_{1,\perp}^\chi + 2q_{2,\perp}^\chi + (2\beta_2 - 4\beta_1)p_b^\chi)] - 4p_a^\tau p_a^\chi g_s^2 \left[\frac{(T^\beta T^\alpha)_{ca}}{\alpha_2 s^2(\alpha_2+\beta_2)} + \frac{(T^\alpha T^\beta)_{ca}}{\alpha_2 s^2(\beta_1-\beta_2)}\right].$$

In the MRK limit, the parameters follow the ordering given in Eq. (2.34). Before applying this approximation, one should take an addition step: a separation of the different Lorentz structures in the expression.

This separation is necessary because, through the eikonal approximation, the subleading momenta have already been neglected. Consequently, the remaining expression can be decomposed into independent Lorentz structures. The function `CollectLorentzStructures[expr_]` performs exactly this task — it returns a list containing all distinct Lorentz structures in `expr`.

Once the decomposition is done, the MRK limit can be applied to each Lorentz structure individually. Eq. (2.34) is translated to

$$\alpha_1 = \lambda_1\epsilon, \quad \alpha_2 = \lambda_2\epsilon^2, \quad \beta_1 = \lambda_3\epsilon^2, \quad \beta_2 = \lambda_4\epsilon, \tag{3.18}$$

where each λ_i is of order unity and ϵ is a small expansion parameter. The approximation is implemented via `approxByEpsilonHierarchy[expr_, paramHierarchy_List, epsilon_: \[CurlyEpsilon], maxOrder_: 20]`. Here, `paramHierarchy` specifies the relative orders of the parameters in powers of ϵ. For the MRK case above, the list is $\{1, \{\alpha_1, \beta_2\}, \{\alpha_2, \beta_1\}\}$. The function then expands and truncates the result up to the specified `maxOrder`.

While the method described above works well for simple expressions, complications arise when denominators are present. In such cases, the approximation is done to both the numerator and the denominator at their lowest relevant powers of ϵ. `approxRationalByepsilon[expr_, orderHierarchy_List]` implements this through by separating the numerator and denominator of expr, applying the previously introduced approximation routine to each part individually, and then recombining them.

However, this straightforward approach fails when the expression contains a sum of terms with different denominators. In that situation, the procedure must be applied term by term. `Finalapprox[expr_]` checks whether the input is a sum; if so, it applies the approximation separately to each summand and then reconstructs the sum. After applying this process and using the commutation relations of the color structures, one finds, for the $M_\uparrow$ vertex,

$$\Lambda^{\tau\chi}_{ca;\alpha\beta} \approx \frac{2ig_s^2 f^{\alpha\beta\gamma}T^\gamma_{ca}}{\alpha_2\beta_2 s^2(\alpha_2+\beta_1)}[-\beta_2^2 s\eta^{\tau\chi} + \beta_2 p_a^\chi(q_1+q_2)^\tau_\perp - 2\beta_2 q_{1,\perp}^\chi p_a^\tau \tag{3.19}$$
$$+ \beta_2 q_{2,\perp}^\chi p_a^\tau - (\alpha_1\beta_2 + 2\alpha_2 + 2\beta_1)p_a^\tau p_a^\chi + \beta_2^2(p_a^\chi p_b^\tau + p_a^\tau p_b^\chi)].$$

In the amplitude, this vertex is multiplied by $\overline{u}(k_2)\gamma_\chi u(p_b)$. Using Eq. (3.10), one can then multiply by $p_{b,\chi}$ into the effective vertex, enabling further simplifications. Substituting $2s \to p_a^\chi p_{b\chi}$ only once, the result is

$$\Lambda^{\tau\chi}_{ca;\alpha\beta} \approx \frac{4ig_s^2 p_a^\chi f^{\alpha\beta\gamma} T^\gamma_{ca}}{\beta_2 s t'(\alpha_2+\beta_1)} \left[p_a^\tau \left(\alpha_1 - 2\frac{t-t'}{\beta_2} \right) + p_b^\tau \beta_2 - (q_1+q_2)^\tau_\perp \right]. \tag{3.20}$$

This matches the result reported in [12]. Repeating the same procedure for $M_\downarrow$ yields

$$M_\uparrow \approx \frac{4ig_s^2 p_a^\chi p_{b\chi} \epsilon^\tau f^{\alpha\beta\gamma} T^\gamma_{ca} T^\alpha_{db}}{s t'(\alpha_2+\beta_1)} \left[p_a^\tau \left(\alpha_1 - 2\frac{t-t'}{s\beta_2} \right) + p_b^\tau \beta_2 - (q_1+q_2)^\tau_\perp \right]; \tag{3.21}$$

$$M_\downarrow \approx \frac{4ig_s^2 p_a^\chi p_{b\chi} \epsilon^\tau f^{\alpha\beta\gamma} T^\alpha_{ca} T^\gamma_{db}}{s t(\alpha_2+\beta_1)} \left[p_a^\tau \alpha_1 + p_b^\tau \left(\beta_2 - 2\frac{t'-t}{s\alpha_1} \right) - (q_1+q_2)^\tau_\perp \right]. \tag{3.22}$$

Combining both amplitudes gives the effective vertex for two Reggeized gluons and one normal gluon. To perform this combination, it is necessary to manipulate the dummy indices in the color structures. In particular, the use of the identity

$$f^{\alpha\beta\gamma} T^\gamma_{db} T^\alpha_{ca} = -f^{\alpha\beta\gamma} T^\alpha_{db} T^\beta_{ca}, \tag{3.23}$$

is needed. The complete amplitude takes the form

$$M = \epsilon_\tau(k) \left(\frac{2g_s p_a^\chi T^\gamma_{ca}}{t} \right) \Gamma^\tau_{\chi\sigma} f^{\alpha\beta\gamma} \left(\frac{2g_s p_b^\sigma T^\alpha_{db}}{t'} \right), \tag{3.24}$$

where

$$\Gamma^\tau_{\chi\sigma} = ig_s \eta_{\chi\sigma} \left[p_a^\tau \left(\alpha_1 - 2\frac{t}{\beta_2 s} \right) + p_b^\tau \left(\beta_2 - 2\frac{t'}{\alpha_1} \right) - (q_1+q_2)^\tau_\perp \right]. \tag{3.25}$$

Diagramatically, this is given by

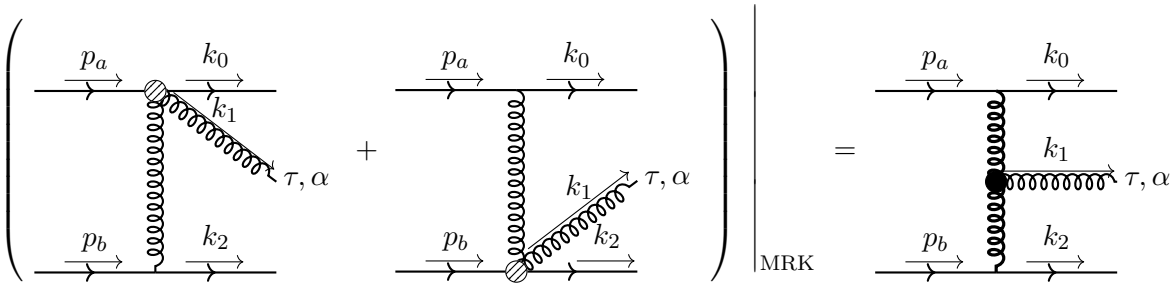

This is precisely the result that we were looking for. It will be discussed further in the next section.

3.2 Gravity Vertex

This section is focused on the computation of the process of the graviton radiation from the interaction of two distinguishable scalars. The diagrams shown in Fig. 1 were present for this process.

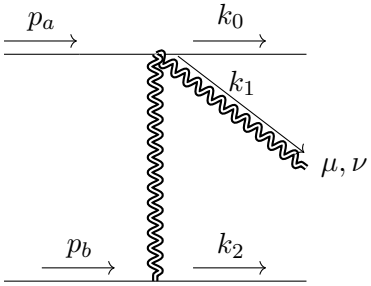

(a) Diagram with the vertex of two scalars and two gravitons in the upper part.

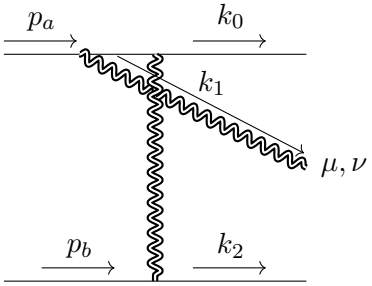

(b) Diagram where the upper scalar has an initial bremsstrahlung.

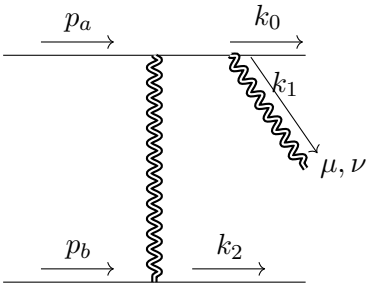

(c) Diagram where the upper scalar has a final bremsstrahlung.

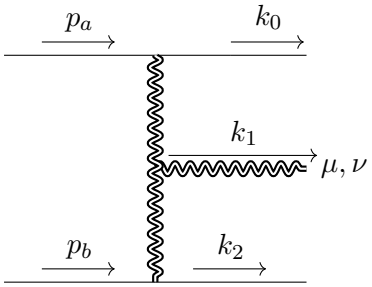

(d) Diagram with the emission of a graviton in the virtual graviton exchange.

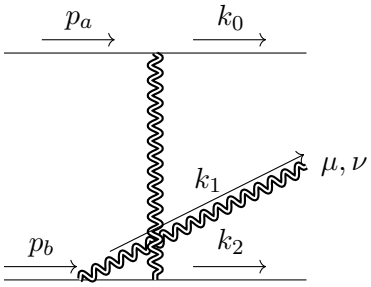

(e) Diagram where the lower scalar has an initial bremsstrahlung.

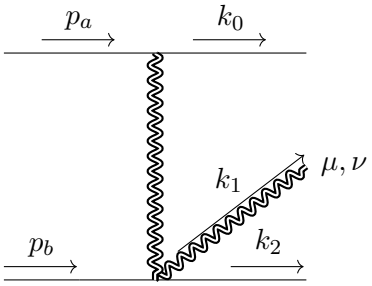

(f) Diagram with the vertex of two scalars and two gravitons in the lower part.

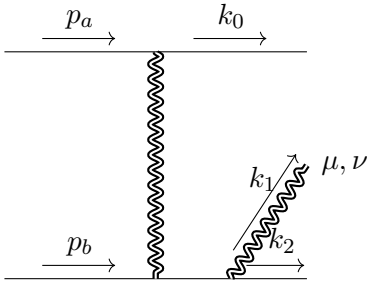

(g) Diagram where the lower scalar has a final bremsstrahlung.

Figure 1: All possible diagrams for the process $SS' \to SS'g$. The corresponding amplitudes are labeled by M_i, where $i = 1, ..., 7$.

Having established the computational framework in QCD, we now apply a similar approach to gravity. Here the emphasis shifts from code implementation to outlining the overall procedure, with only essential coding steps highlighted when relevant. New coding steps are still discussed when relevant, but they are fewer compared to the QCD case. Before proceeding, it will be useful to make a couple of comments about how amplitudes are computed.

As explained in Sect. C, FG works directly by implementing the different elements (propagators, vertices and so on). In this work, two versions of the amplitude were computed: one with the polarization contracted, used for deriving the effective vertex, and one without, used for verifying Gauge Invariance (GI). Proving GI is useful to check possible errors. For this thesis, the procedure played a key role in uncovering possible inconsistencies or missing terms in the FR (see Sect. 1.3.1). Unlike in the QCD case, the complexity of the vertices prevents a manual check, making computer verification essential.

For clarity, the amplitudes contracted with the polarization vectors (used to compute the effective vertex) are denoted by `Mi`, and the amplitudes contracted with the external momentum (used to verify gauge invariance) by `MiGI`. The Ward Identities, which will be used to check the GI, are given by

$$M^{\mu\nu}k_\mu = 0 = M^{\mu\nu}k_\nu, \tag{3.26}$$

where $M = M^{\mu\nu}\epsilon_\mu\epsilon_\nu$, being M the amplitude. Therefore, `MiGI` is already contracted with the momentum. Both amplitudes have been simplified using momentum conservation and the Sudakov parametrization (Eq. (2.35)). Additionally, the on-shell conditions for the polarization, which are given by,

$$\epsilon(k_1)\cdot\epsilon(k_1) = 0; \qquad \epsilon(k_1)\cdot k_1 = 0. \tag{3.27}$$

help to simplify the expressions in `Mi`.

With these simplifications, the results can be reproduced. One of the most interesting feature to extract from QCD are the guage invariant sectors. To replicate this, the following 2 subamplitudes have been defined

$$M_\uparrow = M_2 + M_3 + \frac{t}{t-t'}(M_1 + M_4); \qquad M_\downarrow = M_6 + M_7 - \frac{t'}{t-t'}(M_5 + M_4). \tag{3.28}$$

By summing them together, the full amplitude is recovered, i.e.,

$$M = M_\uparrow + M_\downarrow, \tag{3.29}$$

which in turn implies

$$tM_1 = t'M_5. \tag{3.30}$$

This relation follows from the fact that both vertices—the one with two scalars and a graviton, and the one with two scalars and two gravitons—share the same momentum dependence, namely $p^\mu q^\nu + p^\nu q^\mu$ where p and q are the scalar momenta (see Appendix B). Both, $M_\uparrow$ and $M_\downarrow$ are gauge invariant. Seeing this in the code is precisely the role of `M1GI`. Coding Eqs. (3.28) it was found that

$$M^{\mu\nu}_\uparrow k_\mu = 0; \qquad M^{\mu\nu}_\downarrow k_\mu = 0, \tag{3.31}$$

where $M^{\mu\nu}_{\uparrow/\downarrow}\epsilon_\mu\epsilon_\nu = M_{\uparrow/\downarrow}$. These results confirm the consistency of the calculation up to this stage. Nevertheless, some caution is required: in `M1GI` and `M5GI` an extra factor of 2 arises when implementing the expressions in code (see Sect. 1.3.1 for a detailed discussion). This factor is essential—without it, the gauge invariance condition would not be satisfied. Once the GI is proved, the focus now turns to the effective vertex. With that in mind, the use of Eq. (2.31) will be needed to leave the final expression in terms of p_a, p_b, $q_{1\perp}$ and $q_{2\perp}$. By using Eq. (3.27) one can prove

$$\begin{aligned}\epsilon\cdot q_{1\perp} &= \epsilon\cdot q_{1\perp} - \frac{1}{2}\epsilon\cdot k_1 \\ &= \frac{1}{2}\left(\epsilon\cdot(q_1+q_2)_\perp - (\alpha_1-\alpha_2)\epsilon\cdot p_a - (\beta_1-\beta_2)\epsilon\cdot p_b\right);\end{aligned} \tag{3.32}$$

$$\begin{aligned}\epsilon\cdot q_{2\perp} &= \epsilon\cdot q_{2\perp} + \frac{1}{2}\epsilon\cdot k_1 \\ &= \frac{1}{2}\left(\epsilon\cdot(q_1+q_2)_\perp + (\alpha_1-\alpha_2)\epsilon\cdot p_a + (\beta_1-\beta_2)\epsilon\cdot p_b\right).\end{aligned} \tag{3.33}$$

These relations are useful to symmetrize over $q_{1\perp}$ and $q_{2\perp}$. Without this step, the output would lack the expected symmetry between the two four-vectors. An appropriate example to illustrate this is the lack of any structure with $(q_{1\perp}\cdot\epsilon)^2$ in the output, while $(q_{2\perp}\cdot\epsilon)^2$ is present. The motivation to do this is the fact that the effective vertex in QCD has this kind of symmetry. Consquently, if one is looking for some double copy structure, the symmetry should appear. For convenience, the definition $q_{1\perp}+q_{2,\perp}\equiv q_\perp$ has been used at this point.

With all of this procedure, the exact amplitude, without any approximations has been obtained. Following [12] the amplitude is separated as

$$\begin{aligned}M =& A_{qq}\epsilon\cdot q_\perp\epsilon\cdot q_\perp + A_{p_aq}\epsilon\cdot q_\perp\epsilon\cdot p_a + A_{p_bq}\epsilon\cdot q_\perp\epsilon\cdot p_b + A_{p_ap_a}\epsilon\cdot p_a\epsilon\cdot p_a \\ &+ A_{p_ap_b}\epsilon\cdot p_a\epsilon\cdot p_b + A_{p_bp_b}\epsilon\cdot p_b\epsilon\cdot p_b.\end{aligned} \tag{3.34}$$

At this point, a function similar to `CollectLorentzStructures[expr_]` was used. This function called `CollectByPolStructures[expr_, momList_List]`, collects the different polarizations instead of the Lorentz structures, as was previously done. The reasoning is similar to what was stated before, that the MRK limit will only take place in the coefficients of each structure, not between momenta. It is important to emphasize that, up to this stage, all expressions are exact. While the MRK limit will be introduced shortly, approximations have not yet been necessary. Consequently, the exact coefficients of the polarizations are given by

$$\begin{aligned}A_{p_ap_a} = \frac{i\kappa^3}{16}\Bigg[&\frac{(\alpha_1-\alpha_2)^3}{\alpha_1\alpha_2\beta_1} + \frac{4(\alpha_1-1)(\alpha_1-\alpha_2-1)}{\alpha_2(\beta_2-\beta_1)} - \frac{(\alpha_1-1)(\alpha_1+\alpha_2)^2}{\alpha_1(\alpha_1+\beta_1)} \\ &+ \frac{(\alpha_2-1)(\alpha_1+\alpha_2-2)^2}{\alpha_2(\alpha_2+\beta_2)}\Bigg];\end{aligned} \tag{3.35}$$

$$\begin{aligned}A_{p_bp_b} = \frac{i\kappa^3}{16}\Bigg[&-\frac{(\beta_1-\beta_2)^3}{\alpha_2\beta_1\beta_2} - \frac{4(\beta_2+1)(\beta_1-\beta_2-1)}{\beta_1(\alpha_1-\alpha_2)} - \frac{(\beta_1+1)(\beta_1+\beta_2+2)^2}{\beta_1(\alpha_1+\beta_1)} \\ &+ \frac{(\beta_2+1)(\beta_1+\beta_2)^2}{\beta_2(\alpha_2+\beta_2)}\Bigg];\end{aligned} \tag{3.36}$$

$$A_{p_a p_b} \frac{i\kappa^3}{8} [(\alpha_1+\alpha_2-2)(\beta_1-\alpha_2)+(\alpha_1+\alpha_2)(\alpha_2+\beta_2)] \tag{3.37}$$
$$\times \left[\frac{\alpha_1-\alpha_2}{\alpha_1\alpha_2\beta_1}+\frac{1-\alpha_1}{\alpha_1(\alpha_1+\beta_1)}+\frac{\alpha_2-1}{\alpha_2(\alpha_2+\beta_2)}\right];$$

$$A_{qp_b} = \frac{i\kappa^3}{8}\left[-\frac{(\beta_1-\beta_2)^2}{\alpha_2\beta_1\beta_2}-\frac{(\beta_1+1)(\beta_1+\beta_2+2)}{\beta_1(\alpha_1+\beta_1)}+\frac{(\beta_2+1)(\beta_1+\beta_2)}{\beta_2(\alpha_2+\beta_2)}\right]; \tag{3.38}$$

$$A_{qp_a} = \frac{i\kappa^3}{8}\left[-\frac{(\alpha_1-\alpha_2)^2}{\alpha_1\alpha_2\beta_1}-\frac{(\alpha_1-1)(\alpha_1+\alpha_2)}{\alpha_1(\alpha_1+\beta_1)}+\frac{(\alpha_2-1)(\alpha_1+\alpha_2-2)}{\alpha_2(\alpha_2+\beta_2)}\right]; \tag{3.39}$$

$$A_{qq} = \frac{i\kappa^3}{16}\left[\frac{1}{\beta_1\alpha_2}-\frac{1+\beta_1}{\beta_1(\alpha_1+\beta_1)}-\frac{1-\alpha_2}{\alpha_2(\alpha_2+\beta_2)}\right]. \tag{3.40}$$

Presenting the amplitudes in this way also provides an additional consistency check. By unitarity, the amplitude cannot exhibit simultaneous singularities or multiple poles in the energy variables, a condition known as the Steinmann relations. In the present case, the relevant energy variables are

$$s_{01} = -\hat{s}(\alpha_2+\beta_2); \qquad s_{23} = \hat{s}(\alpha_1+\beta_1). \tag{3.41}$$

Thanks to the chosen form of the amplitudes, it is immediately clear that no multiple poles appear in these variables. Although the Steinmann relations were first discussed decades ago ([42, 43]), they have received relatively little attention until recently, and no comprehensive reviews exist. A few works have touched on them ([44, 45]), but none have provided a full discussion. For this reason, further details on the topic are omitted in this thesis.

3.2.1 Gravity Regge Limit

Despite the fact that the results obtained are enough to find some effective vertex, the usage of the MRK limit will greatly simplify things. The logic of this approximation is the same as in the QCD case. Thus, no further detailed is presented. The function `Finalapprox` will be used to approximate all the amplitudes obtained (Eqs. (3.35) - (3.40)). In the previous section, what was approximated were the different Lorentz structures, once the eikonal approximation had already been used. In this case, the use of the eikonal approximation is unnecessary, as the expressions are more intricate and do not yield terms of the type $p_a - k_1$. The approximated amplitudes are

$$A_{p_a p_a} \approx \frac{i\kappa^3}{16\alpha_2\beta_1\beta_2^2}[(\alpha_1\beta_2-2\beta_1)^2+4\alpha_2\beta_1]; \tag{3.42}$$

$$A_{p_b p_b} \approx \frac{i\kappa^3}{16\alpha_1^2\alpha_2\beta_1}[\alpha_1^2\beta_2^2+4\alpha_2(\alpha_1\beta_2+\beta_1)+4\alpha_2^2]; \tag{3.43}$$

$$A_{p_a p_b} \approx \frac{i\kappa^3}{8\alpha_2\beta_1}[\alpha_1\beta_2+2\alpha_2-2\beta_1]; \tag{3.44}$$

$$A_{qp_b} \approx \frac{i\kappa^3}{8\alpha_1\alpha_2\beta_1}[\alpha_1\beta_2+2\alpha_2]; \tag{3.45}$$

$$A_{qp_a} \approx \frac{i\kappa^3}{8\alpha_2\beta_1\beta_2}[2\beta_1-\alpha_1\beta_2]; \tag{3.46}$$

$$A_{qq} \approx \frac{i\kappa^3}{16\alpha_2\beta_1}. \tag{3.47}$$

The final step is to construct an expression analogous to the effective vertex. There are two possible approaches. The first consists of returning to the original amplitudes before polarization

contractions were applied. Starting from this form, one can add a term of the form $k_1^\mu \Lambda^\nu$ to the amplitude; this term vanishes when contracted with the polarization tensor, leaving the physical amplitude unchanged. In this sense, $M^{\mu\nu}$ and $M^{\mu\nu} + k_1^\mu \Lambda^\nu$, differ formally, but are physically equivalent.

The second approach is to start from the current result and remove the polarizations manually. For this purpose, the function `PolToFreeIndices[expr_, inds_List]` was developed. In simple cases such as $(\epsilon\cdot p)^2$, polarizations can be removed directly. In cases like $(\epsilon\cdot p)(\epsilon\cdot q)$, the momenta must be symmetrized, which is implemented via `PolToFreeIndicesSym` using the previous function. This approach has a slight advantage: some manipulations involving the polarization tensor (e.g., Eqs. (3.32) and (3.33)) have already been applied, simplifying the result. Returning to the original amplitudes would require repeating these steps. Once this approach is adopted, the amplitude can be defined as $\mathcal{M} = M/A_{kk}$, which will be discussed further in the next section. From this, one obtains

$$\begin{aligned}\mathcal{M}^{\mu\nu} \approx\ & p_a^\mu p_a^\nu \frac{(\alpha_1\beta_2 - 2\beta_1)^2 + 4\alpha_2\beta_1}{\beta_2^2} + (p_a^\mu p_b^\nu + p_a^\nu p_b^\mu)(\alpha_1\beta_2 + 2\alpha_2 - 2\beta_1) + q_\perp^\mu q_\perp^\nu \\ & + p_b^\mu p_b^\nu \frac{(\alpha_1\beta_2 + 2\alpha_2)^2 + 4\alpha_2\beta_1}{\alpha_1^2} + \frac{2\beta_1 - \alpha_1\beta_2}{\beta_2}(p_a^\mu q_\perp^\nu + p_a^\nu q_\perp^\mu) - \frac{\alpha_1\beta_2 + 2\alpha_2}{\alpha_1}(p_b^\mu q_\perp^\nu + p_b^\nu q_\perp^\mu).\end{aligned} \tag{3.48}$$

Which is the effective vertex for the gravitons.

4 Discussion

Having outlined the procedure in the previous section, we now turn to the interpretation of the results, starting with the structure of the vertices.

In the QCD case, the amplitude was decomposed into distinct factors. One of these, $(\Gamma^\tau_{\chi\sigma})$, was identified as the effective vertex for the gluons, while the remaining factors correspond to contributions from the quarks. For instance, the term $2p_a^\chi T^\gamma_{ca}/t$ represents the vertex associated with the coupling of the upper quark to the gluon. It is also important to note that, among the three gluons involved, two are off-shell and can be reggeized.

For the QG amplitudes, the choice to divide by A_{qq} requires some clarification. Each factor A_{ij} depends on the specific process under consideration; for example, if all external states were taken to be gravitons, the explicit expressions would change. However, their ratios remain process independent ([46, 47]). Since the effective QCD vertex carries a factor of unity in $(k_1 + k_2)_\perp$, this motivates dividing by A_{qq} rather than by any other factor.

A comparison between the two vertices will be useful at this point. For the QCD case, the effective vertex was given through $\Gamma^\tau_{\chi\sigma}$(Eq. (3.25)). This formula, together with the structure constant are representative of the gluon vertex. If this effective vertex is written as

$$\Gamma^\tau_{\chi\sigma} = ig_s\eta_{\chi\sigma}\left[p_a^\tau\left(\alpha_1 - 2\frac{t}{\beta_2 s}\right) + p_b^\tau\left(\beta_2 - 2\frac{t'}{\alpha_1}\right) - (q_1+q_2)_\perp^\tau\right] \equiv ig_s g_{\chi\sigma}\Omega^\tau, \tag{4.1}$$

then the part relevant for the double-copy structure is Ω^τ. The double copy is constructed by

squaring Ω^τ, so that the gravity vertex becomes

$$\tilde{\Omega}^{\mu\nu}_{QG} = \Omega^\mu \Omega^\nu. \tag{4.2}$$

This does not follow the Steinmann relations previously mentioned. In the MRK limit the two channels are given by

$$s_{01} = -\hat{s}(\alpha_2 + \beta_2) \approx -\hat{s}\beta_2; \qquad s_{23} = \hat{s}(\alpha_1 + \beta_1) \approx \hat{s}\alpha_1. \tag{4.3}$$

Thus, having a term proportional to $\frac{1}{\alpha_1\beta_2}$ means a nonphysical pole. These kinds of poles are present in the naive double-copy structure that has been constructed (Eq. (4.2)). This is seen directly by taking a look at the cross terms with p_a^χ and p_b^τ, as they both have one term that go like $1/\alpha_1$ and $1/\beta_2$ respectively. This was solved by Lipatov ([34]) who introduced subtraction terms to fulfill the Steinmann relations. The introduction of a four-vector that was added in a similar way to $\tilde{\Omega}^{\mu\nu}_{QG}$ as

$$\Omega^{\mu\nu}_{QG} = \tilde{\Omega}^{\mu\nu}_{QG} - \mathcal{N}^\mu \mathcal{N}^\nu, \tag{4.4}$$

ensured that the Steinmann relations were satisfied. The four vector is given by

$$\mathcal{N}^\mu = 2\sqrt{k_1^2 k_2^2}\left(\frac{p_a^\mu}{s_{01}} - \frac{p_b^\mu}{s_{23}}\right) \approx -2i\sqrt{\beta_1\alpha_2}\left(\frac{p_a^\mu}{\beta_1} + \frac{p_b^\mu}{\alpha_2}\right). \tag{4.5}$$

A further check can be made by comparing Eq. (3.48) and Eq. (4.2). By a direct comparison, one can see that they do not match. Nonetheless, once the four vectors are included, i.e., once the comparison is done with Eq. (4.4) instead of Eq. (4.2), it was be seen that the double copy does in fact match the result obtained. Moreover, the results obtained match the ones in [12], up to the factors discussed in Sect. 1.3.1.

It is worth emphasizing that the effective vertices obtained are universal, meaning they do not depend on the choice of external states. For example, if instead of using $qq' \to qq'g$ it was used $gg \to ggg$ the effective vertex for the two Reggeized and the one on-shell gluon, would be the same, as we have previously discussed. The case with only gluons is done in [24].

5 Conclusions

The main objective of this thesis was to find the double copy structure of QCD and QG through some Mathematica libraries, while introducing the necessary background topics. We now review whether the objectives of this thesis were accomplished.

In this thesis I studied the concept of the double copy structure. I examined the interpretation from QFT with the BCJ dualities, as well as the concept arising from string theory with the KLT relations. Moreover, I noted that there is also interest in this structure emerging in SUGRA with $\mathcal{N} = 8$, which is conjectured to be renormalizable, though this has yet to be proven. In addition, I have briefly analyzed how gravity is quantized by means of perturbation theory. The main problems encountered were also presented and explained thoroughly.

An analysis about the concept of resummation arising from hadron scattering at high ener-

gies was also carried out. In such scattering, I identified the various elements that parametrize the scattering, and how $\alpha_s \ln(s/Q^2)$ is of order unity, and thus needs to be resummed. I connected this resummation with the Feynman diagrams, and how it is done in QCD. With this, the summation of all the diagrams contributing at LLO have been taken into account, and the gluon propagator has been modified to the so-called Reggeized gluon. I also examined how this is done with the graviton, and the problems arising from additional contributions dominating over the trajectory. In this context of the resummation at high energies, I have also presented the MRK limit, which orders the outgoing particles through its momenta. This limit has been of much use through the calculations. I have also introduced the well known Sudakov parametrization as well as the eikonal approximation.

I studied in detail the computation of the five-point amplitude in both QCD and QG. By applying the MRK and eikonal limits when appropriate, effective vertices were identified: in QCD, the vertex involving two quarks and two gluons, and in QG, the vertex involving two scalars and two gravitons. By combining these vertices, an effective vertex connecting two off-shell and one on-shell gluon (or graviton) was obtained. Throughout the analysis, I documented how each step was implemented within the Mathematica libraries that I developed for this work. It was stated that the resulting effective vertices are universal, as they do not depend on the nature of the external particles. While these results were already known in the literature, they had previously been derived through more cumbersome procedures. The implementation of dedicated Mathematica code allowed the same computations to be performed much more efficiently, and this constitutes the original contribution of the thesis.

Finally, the double copy structure was discussed. It was found that the naive double copy structure did not work properly since it does not follow the Steinmann rules. This has been previously solved, and I have commented that it is done by introducing a subtraction term. Once this term is introduced, we can see that the double copy structure does indeed work for EH gravity and QCD. The results have been reproduced with a code that enables a faster computation and a possible extension to having two gravitons or gluons in the final state.

In conclusion, the objectives of this thesis were successfully achieved, and the methods developed here provide a solid foundation for further extensions to more complex amplitudes.

6 Applications and outlook

6.1 Applications

Apart for the great simplification of the amplitudes, there are other uses to these effective vertices. One of them has already been used in this thesis, but as detail some calculations were not explained in detail, it was not seen. It is recognized that the amplitude is analytic in the s-channel, except at some values. These typically come from particle threshold production. Furthermore they also originate some branch cuts. Through Cauchy's integral theorem one finds

$$A(s,t) = \frac{1}{2\pi i}\int_C \frac{A(s',t)}{s'-s} ds', \tag{6.1}$$

where C is a path that do not have any divergences in A(s,t). With this, there is a division of the path such that it does not cross or cut through the poles or the branch cut. Without further detail, which would not bring any insight to the reader for the thesis, the following result is presented

$$A(s,t) = \frac{1}{\pi}\int_{4m^2}^{\infty} \frac{D_s(s',t)}{s'-s} ds' + \frac{1}{\pi}\int_{4m^2}^{\infty} \frac{D_u(u',t)}{u'-u} du' + \text{pole terms}, \tag{6.2}$$

where $D_s(s,t) = \text{Im}\{A(s,t)\}$. These types of relations are the so-called *dispersion relations*. During the proof of Eq. (6.2) the fact that $A(s,t) \xrightarrow{|s|\to\infty} 0$ has been used. This is not always the case. The case such that $A(s,t) \xrightarrow{|s|\to\infty} s^{\lambda}$ being $\lambda > 0$ is a possibility. Were this to be the case, the equation Eq. (6.2) would not be satisfied anymore. Further details of the proof and this general case can be found in [27, 48] and many other books.

However, to gain some profit from this, the computation of the imaginary part is required. This is done through a different procedure. The first of such tools that usually comes to one mind is the optical theorem. However, there is a method that is even more useful. They are called the Cutkosky rules ([49]), and are based on unitarity. They are somewhat similar to the optical theorem, and are just 3 simple steps to obtain the imaginary part of an amplitude at the loop-level, by knowing the one at the previous loop. All of this is computed at the amplitude level, without needing the cross-section, contrary to the optical theorem. However, as the aim of this thesis does not involve any process that needs of them, we will not give more detail.

By combining both, the results of this thesis and this procedure, one should be able to compute some amplitudes easier. These simplifications will come to both theories, QCD and gravity. It may not be able to simplify much, as other techniques would proof to be of more use, but it is remarkable to state this.

6.2 Outlook

The results presented in this thesis suggest several possible directions for future work:

1. **Reproducing other known amplitudes.** An immediate extension would be to reproduce other scattering processes already studied in the literature, such as $gg \to ggg$ ([24]), using the code developed in this thesis as a basis. This would provide a useful cross-check of the implementation and pave the way for tackling more complex processes.

2. **Extension to higher-point amplitudes.** A natural continuation of this work is the computation of six-point amplitudes in the Regge limit. Such a case has not yet been fully computed, and it presents significant technical challenges. The main difficulty arises from the length of the Feynman rules and the large number of diagrams involved. In fact, for the six-point function we estimate around 60 diagrams, which would need to be implemented manually, in contrast to the 7 diagrams treated in this thesis. While this task is possible, it is extremely tedious and motivates the search for more efficient methods.

3. **Towards a dedicated `FeynArts` library for quantum gravity.** Given the obstacles mentioned above, an appealing alternative would be to extend `FeynArts` by creating a library specifically tailored for quantum gravity. Such a development would significantly reduce the burden of implementing diagrams by hand and would allow one to exploit the

automated generation and organization of amplitudes that `FeynArts` already provides for gauge theories. This would not only simplify the computation of six-point amplitudes but also make higher-point and more general processes tractable within the same framework.

In summary, exploring new scattering processes, extending the present work to six-point amplitudes and developing a quantum-gravity implementation for `FeynArts` represent natural and promising directions for future research.

A QCD Feynman Rules

The Feynman Rules of QCD are widley known and can be found in many references([41]). Here we will just list them. The quarks propagator reads as follows where A and B are color indices

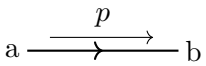

$$\Longrightarrow \qquad \frac{\delta_{ab} i}{\not{p} + i\epsilon}$$

in the fundamental representation. The graviton propagator has the form of

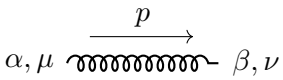

$$\Longrightarrow \qquad -\frac{\delta_{\alpha\beta} i}{p^2 + i\epsilon}\left[\eta_{\mu\nu} + (\xi - 1)\frac{p_\mu p_\nu}{p^2}\right]$$

and now a and b are the color indices in the adjoint representation.

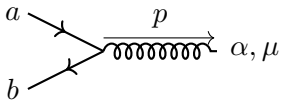

$$\Longrightarrow \qquad ig\gamma_\mu T^\alpha_{ab}$$

where T^α_{ab} are the color generators. The three gluon vertex is given by

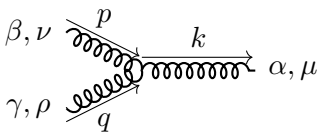

$$\Longrightarrow \qquad gf^{\alpha\beta\gamma}(g^{\mu\nu}(k-p)^\rho + g^{\nu\rho}(p-q)^\mu + g^{\rho\mu}(q-k)^\nu)$$

where $f^{\alpha\beta\gamma}$ are the structure constants of the color group.

B EH gravity Feynman Rules

The FR for the Einstein Hilbert Lagrangian have been obtained directly from the code. As stated in Sect. 1.3.1 they have also been checked in other references ([12, 16, 17, 18]) to ensure that the conventions were safely assumed. All the FR that we are going to state are obtained from $\kappa^2 = 32\pi G_N$. The graviton propagator is given by

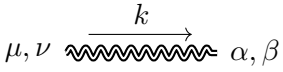

$$\Longrightarrow \qquad i\frac{\eta_{\mu\alpha}\eta_{\nu\beta} + \eta_{\mu\beta}\eta_{\nu\alpha} - \eta_{\mu\nu}\eta_{\alpha\beta}}{2k^2}$$

The scalar propagator is given by

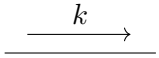

$$\Longrightarrow \qquad \frac{i}{k^2}$$

The vertex between two scalars and a single graviton is given by

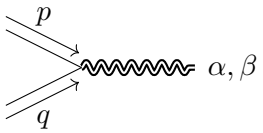

$$\Longrightarrow \qquad -\frac{i\kappa}{2}(p^\mu q^\nu + p^\nu q^\mu)\left(-\eta^{\mu\alpha}\eta^{\nu\beta} + \tfrac{1}{2}\eta^{\mu\nu}\eta^{\alpha\beta}\right)$$

The interaction between two scalars and two gravitons is given by

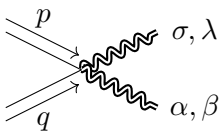

$$\begin{aligned}\Longrightarrow \qquad & -\frac{i\kappa^2}{4}(p^\mu q^\nu + p^\nu q^\mu)(\mathcal{I}^{\alpha\beta}_{\rho\xi}\mathcal{I}^{\sigma\lambda}_{\delta\gamma} + \mathcal{I}^{\alpha\beta}_{\delta\gamma}\mathcal{I}^{\sigma\lambda}_{\rho\xi}) \\ & \times \Big[2\eta^{\gamma\nu}\eta^{\xi\delta}\eta^{\mu\rho} - \eta^{\gamma\nu}\eta^{\mu\delta}\eta^{\rho\xi} \\ & + \eta^{\mu\nu}\left(-\tfrac{1}{2}\eta^{\xi\gamma}\eta^{\rho\delta} + \tfrac{1}{4}\eta^{\delta\gamma}\eta^{\rho\xi}\right)\Big]\end{aligned}$$

For the case of 2 scalars and 2 gravitons we have the symmetrizer

$$I_{\alpha\beta;\gamma\delta} = \frac{1}{2}(\eta_{\alpha\gamma}\eta_{\beta\delta} + \eta_{\alpha\delta}\eta_{\beta\gamma})$$

was introduced. Finally, the coupling between 3 gravitons is given by

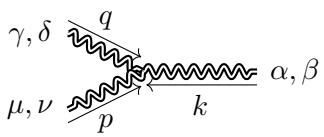

$$\begin{aligned}\Longrightarrow \qquad & 2i\kappa(p_\sigma q_\lambda \mathcal{I}^{\mu\nu}_{\xi\epsilon}\mathcal{I}^{\gamma\delta}_{\rho\chi}\mathcal{I}^{\alpha\beta}_{\tau\nu} + p_\lambda q_\sigma \mathcal{I}^{\gamma\delta}_{\xi\epsilon}\mathcal{I}^{\mu\nu}_{\rho\chi}\mathcal{I}^{\alpha\beta}_{\tau\nu} \\ & + k_\sigma q_\lambda \mathcal{I}^{\mu\nu}_{\xi\epsilon}\mathcal{I}^{\alpha\beta}_{\rho\chi}\mathcal{I}^{\gamma\delta}_{\tau\nu} + k_\lambda q_\sigma \mathcal{I}^{\alpha\beta}_{\xi\epsilon}\mathcal{I}^{\mu\nu}_{\rho\chi}\mathcal{I}^{\gamma\delta}_{\tau\nu} \\ & + k_\sigma p_\lambda \mathcal{I}^{\gamma\delta}_{\xi\epsilon}\mathcal{I}^{\alpha\beta}_{\rho\chi}\mathcal{I}^{\mu\nu}_{\tau\nu} + k_\lambda p_\sigma \mathcal{I}^{\alpha\beta}_{\xi\epsilon}\mathcal{I}^{\gamma\delta}_{\rho\chi}\mathcal{I}^{\mu\nu}_{\tau\nu}) \\ & \times \mathcal{G}^{\lambda;\xi\epsilon;\sigma;\rho\chi;\tau\nu}\end{aligned}$$

where

$$\begin{aligned}\mathcal{G}^{\lambda;\xi\epsilon;\sigma;\rho\chi;\tau\nu} = & -\frac{1}{2}\eta^{\xi\tau}\eta^{\lambda\chi}\eta^{\epsilon\sigma}\eta^{\rho\nu} - -\frac{1}{4}\eta^{\xi\tau}\eta^{\lambda\sigma}\eta^{\epsilon\nu}\eta^{\rho\chi} + \frac{1}{4}\eta^{\xi\sigma}\eta^{\lambda\chi}\eta^{\epsilon\rho}\eta^{\tau\nu} - \frac{1}{8}\eta^{\xi\rho}\eta^{\lambda\sigma}\eta^{\epsilon\chi}\eta^{\tau\nu} \\ & - \eta^{\xi\chi}\eta^{\lambda\rho}\eta^{\epsilon\nu}\eta^{\tau\sigma} + \frac{1}{2}\eta^{\xi\tau}\eta^{\lambda\sigma}\eta^{\epsilon\rho}\eta^{\chi\nu} + \frac{1}{4}\eta^{\xi\rho}\eta^{\lambda\nu}\eta^{\tau\sigma}\eta^{\chi\epsilon} + \frac{1}{2}\eta^{\xi\epsilon}\eta^{\lambda\rho}\eta^{\sigma\nu}\eta^{\chi\tau}\end{aligned} \tag{B.1}$$

Comparing this with FG, one can see that the result is not exactly the same. There appear some extra factors that vanish once the vertex is imposed in any kind of diagram. Also note that this last FR consist of $6 \cdot 2^3 \cdot 8 = 384$ terms, which is incredibly long to be in a simple gauge.

C FeynCalc, FeynArts & FeynGrav

In this section, I will be explaining how to construct diagrams at tree level through the FC, FA and FG libraries in Mathematica [36, 37, 38, 40, 39, 19, 20, 21].

C.1 Basic elements in FeynCalc

Let us first start with the thing that all the codes have

```
1  description="El Ael -> El Ael, QED, matrix element squared, tree";
2  If[ $FrontEnd === Null,
3  $FeynCalcStartupMessages = False;
4  Print[description];
5  ];
6  If[ $Notebooks === False,
7  $FeynCalcStartupMessages = False
8  ];
9  $LoadAddOns={"FeynArts"};
10 <<FeynCalc`
11 $FAVerbose = 0;
12
13 FCCheckVersion[9,3,1];
```

Listing 1: First part of the FeynCalc code.

In this part, we have put a description in the notebook, in the first line. In the lines 2-5 makes sure that we are working on a text-based Mathematica environment. The lines 6-8 checks if the notebooks are disabled. Line 9 and 10 load the packages FA and FC respectively. Notice that they are imported differently. We do it this way, as the FA and FC packages have some terms in common that may collide and generate problems. To avoid such problems, we are importing FA only when it is necessary with the command `LoadAddOns`. Line 11 makes sure that we have a minimal return of messages from the package FA. Finally, line 13 checks that we are working with the correct version of the package FC. Let us now work the common process of creating diagrams at tree-level in QED and QCD, and then we will jump to the one-loop case for both of them.

C.2 QED

The firs thing we always find is the part of the code 2. This is just to make the writting nicer, in case we happen to find some momenta with indices.

```
1  MakeBoxes[p1,TraditionalForm]:="\!\(\*SubscriptBox[\(p\), \(1\)]\)";
2  MakeBoxes[p2,TraditionalForm]:="\!\(\*SubscriptBox[\(p\), \(2\)]\)";
3  MakeBoxes[k1,TraditionalForm]:="\!\(\*SubscriptBox[\(k\), \(1\)]\)";
4  MakeBoxes[k2,TraditionalForm]:="\!\(\*SubscriptBox[\(k\), \(2\)]\)";
```

Listing 2: For a nicer writting of the momenta.

The next step is to create diagrams. Let us see the code that we have to input and then analyse it with detail. For the case of a Babba scattering, i.e., $e^-e^+ \to e^-e^+$, we use the code shown in 3.

```
diags = InsertFields[CreateTopologies[0, 2 -> 2], {F[2, {1}], -F[2, {1}]} -> {
  F[ 2, {1}], -F[2, {1}]}, InsertionLevel -> {Classes}, Restrictions->QEDOnly
  ];
```

Listing 3: To find all the possible diagrams for a given interaction.

The command `InsertFields` has lots of options. First of all, we have the command `CreateTopologies [l, n -> m]` which creates all possible topologies in a process of l loops with n initial particles and m final particles. Then we need to specify the type of particles for the process. We have different levels at which we can specify, which are `Generic`, `Classes` and `Particles`. These are the field levels of FA, and the difference is at which point do we want to specify the type of particles we are working with. The `Generic` level specifies whether the particles are Fermions (`F`), Vectors (`V`), Scalars (`S`), ghost (`U`) or Tensors (`T`). Then, each different generic field has its class. For example `F[2]` is the class of fermions e, μ, τ. Then, the last part is specifying which field we are working with, if electrons, muons or tauons. This is done with `F[2,{1}]`, and the positron, i.e., the anti-electron, is specified with `-F[2,{1}]`. If instead of `F[2]` we have `F[3]` and `F[4]` are the quarks up, strange and top, and down, charm and bottom, respectively. Then we have the `InsertionLevel`, which just tells us at what level do we classify the inner particles that the interaction produces. For example, if we have an `InsertionLevel` of `Generic`, and our mediator is a photon, it will appear as V, i.e., a vector, whereas if we have the `InsertionLevel` of `Classes` or `Particles` it would appear as a photon, i.e., γ. Finally, we have the `Restriction`, which takes into account what kind of interactions can appear. In the case of QED we only find particles that appear in the QED Lagrangian, such as photons, electrons, quarks and all of the particles with electric charge. We have some other features that do not appear, right now, but may be useful in the future. These features include things such as the `GenericModel` we use for the space time, which is Lorentz if not specified any other. In addition, we have `Model`, which specifies the Lagrangian we are working on. Unless specified, we are working with Standard Model (SM). We can also have the feature of `ExcludeFieldPoints`, which basically consists on removing certain kind of interactions between particles. Moreover, the feature `ExcludeParticles` which consists of not including particles for the internal lines, is also available. Finally, we also have the option of `LastSelections`, which enables us to choose field patterns that must or must not appear in the final output.

Immediatly after this, we would put the lines of code that appear in 4.

```
Paint[diags, ColumnsXRows -> {2, 1}, Numbering -> Simple, SheetHeader->None,
  ImageSize->{512,256}];
```

Listing 4: To draw all the diagrams previously found.

The first thing we need to put is the diagrams we have computed previously. Then we need to specify what is the output that we want in the format of rows and columns. For that we have the option `ColumnsxRows`. Then the `Numbering` has various options. The `Simple` just enumerates the different diagrams. We also have the option of `Full`, which tells us three things. First of all the topology, followed by different options, which are ghosts, class or propagator, depending on which `InsertionLevel` we are at. They correspond to the levels `Generic`, `Classes` and, `Particles` respectively. Finally, we also have the number of nodes. With all of this, assuming that we have an `InsertionLevel` of `Generic`, we would see, for example, the numbering `T1 G1 N1` for a given

diagram. Finally, we have the option `Numbering -> None`, if we just do not want any numbering. Finally, we have the options of `SheetHeader` and `ImageSize`, which describe themselves. Some other options are available, but we will not mention them here as I think that they are important enough right now. If they are in the future, I will make sure to describe what its function is.

Then we need to compute the amplitude. To do so we use the following code lines 5.

```
Clear[amp]
amp[_] =.;  (* Define amp as an indexed symbol *)
amp[0] = FCFAConvert[CreateFeynAmp[diags], IncomingMomenta->{p1,p2},
  OutgoingMomenta-> {k1,k2},UndoChiralSplittings->True,ChangeDimension->4,
  List->False, SMP->True, Contract->True]
```

Listing 5: How to compute the amplitude of the diagrams we have obtained.

The line `Clear[amp]` makes sure that, if amp was defined before, now it is free to use. Then we have the command `amp[_]` which defines `amp` as a vector. The usefulness of this, will become clear in the future. Finally, we have the command `FCFAConvert`, which basically converts from FA into FC. This comes with lots of different options. The option `CreateFeynAmp` speaks for itslef. Then we define the incoming and outgoing momenta through `IncomingMomenta->{p1,p2}` and `OutgoingMomenta-> {k1,k2}`. Afterwards, we would encounter with `UndoChiralSplittings`. This option basically puts together all the possible chiral projectors, and with that I mean that if we have $aP_R + aP_L$ this would become a. Then we have the command `ChangeDimension`, which specifies the change of dimension, as previously we were working in a generic dimension. Then, `List -> False` what does is return the amplitudes in a sum instead of a list. Were `List -> True` to be, then we would find an output of $\{\mathcal{M}_1, \mathcal{M}_2\}$ instead of $\mathcal{M}_1 + \mathcal{M}_2$. Then we have the `SMP` command, which basically uses the SM definitions for couplings, masses and any other constant needed. Finally, `Contract`, basically contracts all the possible indices in the amplitudes.

Then, we have to set the Mandelstav variables for commodity with the code 6.

```
FCClearScalarProducts[];
SetMandelstam[s, t, u, p1, p2, -k1, -k2, SMP["m_e"], SMP["m_e"], SMP["m_e"],
  SMP["m_e"]];
```

Listing 6: Setting the Mandelstav variables to have a more compact result.

Then, we square the amplitudes with the code 7.

```
ampSquared[0] = (amp[0] (ComplexConjugate[amp[0]]))//
  FeynAmpDenominatorExplicit//FermionSpinSum[#, ExtraFactor -> 1/2^2]&//
  DiracSimplify//Simplify
```

Listing 7: Squaring the amplitude and simplifying things.

The commands are very explicit, and talking about how they work might be useless, so we will skip it. The only thing worth to mention is what `//` and `//&` do. This is more of a Mathematica thing, but we will also make a brief comment. The `//` basically applies the function to the right, to the expression of the left. The function `//&` is very similar, but in the right we find an expression with a `#`. This means that whatever is on the left, will be substituted in place of the `#` on the expression on the right.

In addition to what we computed previously, we can take the massless limit with the code 8.

```
ampSquaredMassless[0] = ampSquared[0]//ReplaceAll[#,{SMP["m_e"] -> 0}]&//
  Simplify
```

Listing 8: Taking the limit of the mass going to 0.

Last but not least, we can compare with a known result, if available, through the code 9.

```
knownResult = (2 SMP["e"]^4 (s^2+u^2)/t^2 + 4 SMP["e"]^4 u^2/(s t) + 2 SMP["e
  "]^4 (t^2+u^2)/s^2);
FCCompareResults[ampSquaredMassless[0],knownResult,
Text->{"\tCheck the final result:", "CORRECT.","WRONG!"}, Interrupt->{Hold[
  Quit[1]],Automatic}];
Print["\tCPU Time used: ", Round[N[TimeUsed[],4],0.001], " s."];
```

Listing 9: Comparing with a known result.

This code also prints the time it has taken to compute all of this. Now we will present the same scattering, but in one loop, and we will comment in which part need to be changed.

C.3 QCD

This code is very similar to the one of QED, so we will just quickly comment on the different changes. In order to make a comparison, we work with the scattering of two different quarks. They start by looking at how the diagrams are created. If we look at the code 10, we see that the first difference appears when we introduce the particles, but this is a trivial one, as we are dealing with a different process. Then, we find that instead of using the command, `Restrction`, we are using the command `Model` to pick the Lagrangian we are working on. This is something that we already commented on before. On top of that, now we are excluding the particles, `V[12]`—, which are just the photon and the Z boson. The particles `S[_]` are all the scalars of the SM, which are the High's boson and the Goldstones.

```
diags = InsertFields[CreateTopologies[0, 2 -> 2],  {F[3, {1}], F[3, {2}]} ->
{F[3, {1}], F[3, {2}]}, InsertionLevel -> {Classes}, Model -> "SMQCD",
ExcludeParticles -> {S[_],V[1|2]}];

Paint[diags, ColumnsXRows -> {2, 1}, Numbering -> Simple,
SheetHeader->None,ImageSize->{512,256}];
```

Listing 10: Creating diagrams with QCD for an interaction of two quarks.

For the amplitude, we would find something very similar also, but with a slight change.

```
amp[0] = FCFAConvert[CreateFeynAmp[diags], IncomingMomenta->{p1,p2},
OutgoingMomenta->{k1,k2},UndoChiralSplittings->True,ChangeDimension->4,
List->False, SMP->True, Contract->True,DropSumOver->True]
```

Listing 11: Computing the amplitude in QCD at tree level.

The only difference in the code 11 is the command `DropSumOver`. This is just done to obtain a result more clear, and all it does is to drop the terms `SumOver` of what we see. This is done as

Einstein convention usually applies, and it may help us see the final result way more clear.

Finally, we would have also to change the Mandesltam variables, as now the different particles may have different masses. However, as this is trivial, we will not write anything about it.

When squaring the amplitudes, we start to find more differences when comparing to the QED case.

```
ampSquared[0] = 1/(SUNN^2)(amp[0] (ComplexConjugate[amp[0]]))//
FeynAmpDenominatorExplicit//SUNSimplify[#,Explicit->True,
SUNNToCACF->False]&//FermionSpinSum[#, ExtraFactor -> 1/2^2]&//
DiracSimplify//TrickMandelstam[#,{s,t,u,2SMP["m_u"]^2+2SMP["m_c"]^2}]&//
  Simplify
```

Listing 12: Computing the squared amplitude in QCD at tree level.

The first thing we notice in the code 12 is the command `SUNN`. This just denotes the total number of colors, N. Then, in the command `SUNSimplify` we find the option `SUNNToCACF -> False`. Were this to be `True`, one would just find the result in terms of the Casimir operators eigenvalues, **CA** and **CF**. Finally, the command `TrickMandelstam` what does is to eliminate of the Mandesltam variables from the expression

$$s + t + u = m_1^2 + m_2^2 + m_3^2 + m_4^2. \tag{C.1}$$

Now, finally, we can also take the massless limit and substitute N with 3. When this is done, we can compare with some known results. All of this is shown in the code 13.

```
ampSquaredMassless[0] = ampSquared[0]//ReplaceAll[#,{SMP["m_u"|"m_c"] ->
  0}]&//
TrickMandelstam[#,{s,t,u,0}]&
ampSquaredMasslessSUNN3[0] = ampSquaredMassless[0]/.SUNN->3
knownResults = {
   ((4/9)SMP["g_s"]^4 (s^2+u^2)/t^2)
};
FCCompareResults[{ampSquaredMasslessSUNN3[0]},{knownResults},
Text->{"\tCompare to Ellis, Stirling and Weber, QCD and Collider Physics, \
   Table 7.1:",
   "CORRECT.","WRONG!"}, Interrupt->{Hold[Quit[1]],Automatic},Factoring->
Function[x,Simplify[TrickMandelstam[x,{s,t,u,0}]]]]
Print["\tCPU Time used: ", Round[N[TimeUsed[],3],0.001], " s."];
```

Listing 13: Final steps for a tree level scattering in QCD.

C.4 QG

Working with FG is somewhat easier to understand than FC and FA. At least it has a more direct way of computing the diagrams. The idea behind FG is that the details of the diagram have to be specified. This is a procedure similar to do it by hand. The first step to do is import the FG library through `<<FeynGrav‘`. The example given is the t-channel of the scattering of two different scalars, which is given in Code. 14

```
SetMandelstam[s, t, u, p1, p2, k0, k2, 0, 0, 0, 0];
```

```
Ms[p1_, p2_, k1_, k2_] = Calc[GravitonScalarVertex[{\[Alpha]1, \[Beta]1}, p1,
  k1, 0]*
FeynAmpDenominatorExplicit[GravitonPropagator[\[Alpha]1, \[Beta]1, \[Alpha]2,
  \[Beta]2, p1-k1]]*
GravitonScalarVertex[{\[Alpha]2, \[Beta]2}, p2, k2, 0]]//Simplify
```

Listing 14: Amplitude of the scattering of two different quarks through the t-channel.

The code is not as difficult to analyse as the QCD one. Here we just have to the vertices through `GravitonScalarVertex[{\[Alpha]1,\[Beta]1, ... \[Alpha]n, \[Beta]n}, p1, k1, m]`. This vertex is used for the interactions between n gravitons and 2 scalars with mass m. The other function is the graviton propagator, which is given by `GravitonPropagator[\[Alpha]1, \[Beta]1, \[Alpha]2, \[Beta]2, q]`.

All the conservation ofn momenta, checking that the indices match, and so on has to be done by hand. This is not as useful as using FA, but it is better than doing things completely by hand. An enormous amount of time is saved by not having to look at the FR, as well as having a program that does it automatically. We could say that this is in the middle between using FA and doing things by hand.

References

[1] Zvi Bern et al. *The Duality Between Color and Kinematics and its Applications*. 2019. arXiv: 1909.01358 [hep-th]. URL: https://arxiv.org/abs/1909.01358.

[2] Zvi Bern et al. "Gravity as the square of gauge theory". In: *Physical Review D* 82.6 (Sept. 2010). ISSN: 1550-2368. DOI: 10.1103/physrevd.82.065003. URL: http://dx.doi.org/10.1103/PhysRevD.82.065003.

[3] Henrik Johansson et al. *Color-kinematics duality and dimensional reduction for graviton emission in Regge limit*. 2013. arXiv: 1310.1680 [hep-th]. URL: https://arxiv.org/abs/1310.1680.

[4] Angel M. Uranga. *Introduction to String theory*. URL: https://members.ift.uam-csic.es/auranga/Lect.pdf.

[5] Tomás Ortín. *Gravity and Strings*. Cambridge Monographs on Mathematical Physics. Cambridge: Cambridge University Press, 2004.

[6] Sidney Coleman and Jeffrey Mandula. "All Possible Symmetries of the S Matrix". In: *Phys. Rev.* 159 (5 July 1967), pp. 1251–1256. DOI: 10.1103/PhysRev.159.1251. URL: https://link.aps.org/doi/10.1103/PhysRev.159.1251.

[7] David Tong. *Supersymmetric Field Theory*. http://www.damtp.cam.ac.uk/user/tong/susy.html. Lecture Notes, Part III Mathematical Tripos. 2005.

[8] Z. Bern et al. "Ultraviolet Behavior of $\mathcal{N} = 8$ Supergravity at Four Loops". In: *Physical Review Letters* 103.8 (Aug. 2009). ISSN: 1079-7114. DOI: 10.1103/physrevlett.103.081301. URL: http://dx.doi.org/10.1103/PhysRevLett.103.081301.

[9] G. Bossard, P. S. Howe, and K. S. Stelle. "The ultra-violet question in maximally supersymmetric field theories". In: *General Relativity and Gravitation* 41.4 (Mar. 2009), pp. 919–981. ISSN: 1572-9532. DOI: 10.1007/s10714-009-0775-0. URL: http://dx.doi.org/10.1007/s10714-009-0775-0.

[10] J. M. Henn and B. Mistlberger. "Four-graviton scattering to three loops in $\mathcal{N} = 8$ supergravity". In: *Journal of High Energy Physics* 2019.5 (May 2019). ISSN: 1029-8479. DOI: 10.1007/jhep05(2019)023. URL: http://dx.doi.org/10.1007/JHEP05(2019)023.

[11] Stephen G. Naculich, Horatiu Nastase, and Howard J. Schnitzer. "Linear relations between $\mathcal{N} \geqslant 4$ supergravity and subleading-color SYM amplitudes". In: *Journal of High Energy Physics* 2012.1 (Jan. 2012). ISSN: 1029-8479. DOI: 10.1007/jhep01(2012)041. URL: http://dx.doi.org/10.1007/JHEP01(2012)041.

[12] Agustin Sabio Vera, Eduardo Serna Campillo, and Miguel A. Vazquez-Mozo. "Graviton emission in Einstein-Hilbert gravity". In: (Dec. 2011). DOI: 10.1007/JHEP03(2012)005. URL: http://arxiv.org/abs/1112.4494%20http://dx.doi.org/10.1007/JHEP03(2012)005.

[13] Zvi Bern, Lance J. Dixon, and David A. Kosower. "$\mathcal{N} = 4$ Super-Yang–Mills theory, QCD and collider physics". In: *Comptes Rendus. Physique* 5.9–10 (Nov. 2004), pp. 955–964. ISSN: 1878-1535. DOI: 10.1016/j.crhy.2004.09.007. URL: http://dx.doi.org/10.1016/j.crhy.2004.09.007.

[14] Alberto Güijosa. "QCD, with strings attached". In: *International Journal of Modern Physics E* 25.10 (Oct. 2016), p. 1630006. ISSN: 1793-6608. DOI: 10.1142/s021830131630006x. URL: http://dx.doi.org/10.1142/S021830131630006X.

[15] Zvi Bern. "Perturbative Quantum Gravity and its Relation to Gauge Theory". In: *Living Reviews in Relativity* 5.1 (July 2002). ISSN: 1433-8351. DOI: 10.12942/lrr-2002-5. URL: http://dx.doi.org/10.12942/lrr-2002-5.

[16] N. E. J. Bjerrum-Bohr, John F. Donoghue, and Barry R. Holstein. "Quantum gravitational corrections to the nonrelativistic scattering potential of two masses". In: *Phys. Rev. D* 67 (8 Apr. 2003), p. 084033. DOI: 10.1103/PhysRevD.67.084033. URL: https://link.aps.org/doi/10.1103/PhysRevD.67.084033.

[17] N. E. J. Bjerrum-Bohr, John F. Donoghue, and Barry R. Holstein. "Quantum corrections to the Schwarzschild and Kerr metrics". In: *Phys. Rev. D* 68 (8 Oct. 2003), p. 084005. DOI: 10.1103/PhysRevD.68.084005. URL: https://link.aps.org/doi/10.1103/PhysRevD.68.084005.

[18] Safi Rafie-Zinedine. *Simplifying Quantum Gravity Calculations*. 2018. arXiv: 1808.06086 [hep-th]. URL: https://arxiv.org/abs/1808.06086.

[19] B Latosh. "FeynGrav: FeynCalc extension for gravity amplitudes". In: *Classical and Quantum Gravity* 39.16 (July 2022), p. 165006. ISSN: 1361-6382. DOI: 10.1088/1361-6382/ac7e15. URL: http://dx.doi.org/10.1088/1361-6382/ac7e15.

[20] B. Latosh. "FeynGrav 2.0". In: *Computer Physics Communications* 292 (Nov. 2023), p. 108871. ISSN: 0010-4655. DOI: 10.1016/j.cpc.2023.108871. URL: http://dx.doi.org/10.1016/j.cpc.2023.108871.

[21] Boris Latosh. "FeynGrav 3.0". In: *Computer Physics Communications* 310 (May 2025), p. 109508. ISSN: 0010-4655. DOI: 10.1016/j.cpc.2025.109508. URL: http://dx.doi.org/10.1016/j.cpc.2025.109508.

[22] Alexander Prygarin et al. "All Two-Loop MHV Amplitudes in Multi-Regge Kinematics From Applied Symbology". In: (2012).

[23] Yuri V. Kovchegov and Eugene Levin. "Frontmatter". In: *Quantum Chromodynamics at High Energy*. Cambridge Monographs on Particle Physics, Nuclear Physics and Cosmology. Cambridge University Press, 2023, pp. i–iv.

[24] Vittorio Del Duca. *An introduction to the perturbative QCD pomeron and to jet physics at large rapidities*. 1995. arXiv: hep-ph/9503226 [hep-ph]. URL: https://arxiv.org/abs/hep-ph/9503226.

[25] B. L. Ioffe, V. S. Fadin, and L. N. Lipatov. *Quantum Chromodynamics: Perturbative and Nonperturbative Aspects*. Cambridge Monographs on Particle Physics, Nuclear Physics and Cosmology. Cambridge: Cambridge University Press, 2010. ISBN: 9780521631488.

[26] Yuri L. Dokshitzer et al. *Basics of Perturbative QCD*. Translated by J. Tran Thanh Van. Gif-sur-Yvette, France: Editions Frontières, 1991. ISBN: 978-2-85182-216-3.

[27] José Daniel Madrigal Martínez. "The High Energy Limit of QCD and N=4 SYM and the Effective Action Approach". Tesis doctoral inédita; fecha de lectura: 17-09-2013. PhD thesis. Madrid, Spain: Universidad Autónoma de Madrid, Departamento de Física Teórica, Sept. 2013. URL: http://hdl.handle.net/10486/660212.

[28] J. R. Forshaw and D. A. Ross. *Quantum Chromodynamics and the Pomeron*. Cambridge Lecture Notes in Physics. Cambridge: Cambridge University Press, 1997.

[29] Michael Saavedra. "Applications and Developments in the Effective Field Theory Approach to Forward Scattering in Gauge Theories and Gravity". In: (June 2025). DOI: 10.1184/R1/29281562.v1. URL: https://kilthub.cmu.edu/articles/thesis/

Applications_and_Developments_in_the_Effective_Field_Theory_Approach_to_Forward_Scattering_in_Gauge_Theories_and_Gravity/29281562.

[30] Ira Z. Rothstein and Michael Saavedra. *A Systematic Lagrangian Formulation for Quantum and Classical Gravity at High Energies*. 2024. arXiv: 2412.04428 [hep-th]. URL: https://arxiv.org/abs/2412.04428.

[31] Jochen Bartels, Lev N. Lipatov, and Agustin Sabio Vera. *Double-logarithms in Einstein-Hilbert gravity and supergravity*. 2012. arXiv: 1208.3423 [hep-th]. URL: https://arxiv.org/abs/1208.3423.

[32] Agustín Sabio Vera. *High-energy scattering amplitudes in QED, QCD and supergravity*. 2020. arXiv: 2001.11885 [hep-th]. URL: https://arxiv.org/abs/2001.11885.

[33] Sergey Bondarenko. *Graviton reggeization and high energy gravitational scattering of scalar particles*. 2024. arXiv: 2406.19067 [hep-th]. URL: https://arxiv.org/abs/2406.19067.

[34] L.N. Lipatov. "Graviton reggeization". In: *Physics Letters B* 116.6 (1982), pp. 411–413. ISSN: 0370-2693. DOI: https://doi.org/10.1016/0370-2693(82)90156-3. URL: https://www.sciencedirect.com/science/article/pii/0370269382901563.

[35] Claude Duhr and Zhengwen Liu. "Multi-Regge kinematics and the scattering equations". In: *Journal of High Energy Physics* 2019.1 (Jan. 2019). ISSN: 1029-8479. DOI: 10.1007/jhep01(2019)146. URL: http://dx.doi.org/10.1007/JHEP01(2019)146.

[36] Vladyslav Shtabovenko, Rolf Mertig, and Frederik Orellana. "FeynCalc 9.3: New features and improvements". In: *Computer Physics Communications* 256 (Nov. 2020), p. 107478. ISSN: 0010-4655. DOI: 10.1016/j.cpc.2020.107478. URL: http://dx.doi.org/10.1016/j.cpc.2020.107478.

[37] Vladyslav Shtabovenko, Rolf Mertig, and Frederik Orellana. "New developments in FeynCalc 9.0". In: *Computer Physics Communications* 207 (Oct. 2016), pp. 432–444. ISSN: 0010-4655. DOI: 10.1016/j.cpc.2016.06.008. URL: http://dx.doi.org/10.1016/j.cpc.2016.06.008.

[38] R. Mertig, M. Böhm, and A. Denner. "Feyn Calc - Computer-algebraic calculation of Feynman amplitudes". In: *Computer Physics Communications* 64.3 (1991), pp. 345–359. ISSN: 0010-4655. DOI: https://doi.org/10.1016/0010-4655(91)90130-D. URL: https://www.sciencedirect.com/science/article/pii/001046559190130D.

[39] Vladyslav Shtabovenko, Rolf Mertig, and Frederik Orellana. "FeynCalc 10: Do multiloop integrals dream of computer codes?" In: *Computer Physics Communications* 306 (Jan. 2025), p. 109357. ISSN: 0010-4655. DOI: 10.1016/j.cpc.2024.109357. URL: http://dx.doi.org/10.1016/j.cpc.2024.109357.

[40] Thomas Hahn. "Generating Feynman diagrams and amplitudes with FeynArts 3". In: *Computer Physics Communications* 140.3 (2001), pp. 418–431. ISSN: 0010-4655. DOI: https://doi.org/10.1016/S0010-4655(01)00290-9. URL: https://www.sciencedirect.com/science/article/pii/S0010465501002909.

[41] Michael E. Peskin and Daniel V. Schroeder. *An Introduction to quantum field theory*. Reading, USA: Addison-Wesley, 1995. ISBN: 978-0-201-50397-5, 978-0-429-50355-9, 978-0-429-49417-8. DOI: 10.1201/9780429503559.

[42] O. Steinmann. "Über den Zusammenhang zwischen den Wightmanfunktionen und der retardierten Kommutatoren". In: *Helv. Phys. Acta* 33 (1960), pp. 257–276.

[43] O. Steinmann. "Wightman-Funktionen und retardierten Kommutatoren. II". In: *Helv. Phys. Acta* 33 (1960), pp. 347–371.

[44] Kevin E Cahill and Henry P Stapp. "Optical theorems and steinmann relations". In: *Annals of Physics* 90.2 (1975), pp. 438–514. ISSN: 0003-4916. DOI: https://doi.org/10.1016/0003-4916(75)90006-8. URL: https://www.sciencedirect.com/science/article/pii/0003491675900068.

[45] Simon Caron-Huot et al. "Bootstrapping a Five-Loop Amplitude Using Steinmann Relations". In: *Physical Review Letters* 117.24 (Dec. 2016). ISSN: 1079-7114. DOI: 10.1103/physrevlett.117.241601. URL: http://dx.doi.org/10.1103/PhysRevLett.117.241601.

[46] V.S. Fadin, E.A. Kuraev, and L.N. Lipatov. "On the pomeranchuk singularity in asymptotically free theories". In: *Physics Letters B* 60.1 (1975), pp. 50–52. ISSN: 0370-2693. DOI: https://doi.org/10.1016/0370-2693(75)90524-9. URL: https://www.sciencedirect.com/science/article/pii/0370269375905249.

[47] Yu Yu Balitsky and L N Lipatov. "The Pomeranchuk singularity in quantum chromodynamics". In: *Sov. J. Nucl. Phys.* 28 (1978), pp. 822–829. URL: https://cds.cern.ch/record/401554.

[48] V. Barone and E. Predazzi. *High-energy particle diffraction*. Springer, 2002.

[49] R. E. Cutkosky. "Singularities and Discontinuities of Feynman Amplitudes". In: *Journal of Mathematical Physics* 1.5 (1960), pp. 429–433. DOI: 10.1063/1.1703676. URL: https://doi.org/10.1063/1.1703676.